



JOURNAL OF **EMERGING INVESTIGATORS**

VOLUME 2, ISSUE 6 | JUNE 2019
emerginginvestigators.org

Far-Off Worlds

Measuring exoplanet properties
using transit photometry

Cemetery crawlers

Analyzing soil microhabitats in historical gravesites

A close look at tea

Comparing the compounds in different tea varieties

DNA damage from UV radiation

Can antioxidants help keep our genetic material safe?

Caffeinated flatworms

Investigating caffeine's impact on regeneration and healing



JOURNAL OF EMERGING INVESTIGATORS

The Journal of Emerging Investigators is an open-access journal that publishes original research in the biological and physical sciences that is written by middle and high school students. JEI provides students, under the guidance of a teacher or advisor, the opportunity to submit and gain feedback on original research and to publish their findings in a peer-reviewed scientific journal. Because grade-school students often lack access to formal research institutions, we expect that the work submitted by students may come from classroom-based projects, science fair projects, or other forms of mentor-supervised research.

JEI is a non-profit group run and operated by graduate students, postdoctoral fellows, and professors across the United States.

EXECUTIVE STAFF

Mark Springel **EXECUTIVE DIRECTOR**
Haneui Bae **COO**
Qiyu Zhang **TREASURER**
Michael Mazzola **DIRECTOR OF OUTREACH**

BOARD OF DIRECTORS

Sarah Fankhauser, PhD
Katie Maher, PhD
Tom Mueller
Brindha Muniappan, PhD
Lincoln Pasquina, PhD
Seth Staples
Jason Tse

EDITORIAL TEAM

Jamilla Akhund-Zade **EDITOR-IN-CHIEF**
Olivia Ho-Shing **EDITOR-IN-CHIEF**
Michael Marquis **EDITOR-IN-CHIEF**
Brandon Sit **MANAGING EDITOR**
Laura Doherty **MANAGING EDITOR**
Michelle Frank **HEAD COPY EDITOR**
Sonia Kim **HEAD COPY EDITOR**
Naomi Atkin **HEAD COPY EDITOR**
Alexandra Was, PhD **PROOFING MANAGER**
Erika J. Davidoff **PUBLICATION MANAGER**

SENIOR EDITORS

Kiana Mohajeri Chris Schwake
Laura Doherty Kathryn Lee

**FOUNDING
SPONSORS**



Contents

VOLUME 2, ISSUE 6 | JUNE 2019

- Measuring exoplanetary radii using transit photometry** 4
Sarah Tiang and William Waalkes
Fairview High School, Boulder, CO
- An analysis of soil microhabitats in Revolutionary War, Civil War, and modern graveyards on Long Island, NY** 9
Dominick Caputo, Jason Rattansingh, Victoria Hernandez, and Bruce Nash, William Floyd High School, Long Island, NY
- A temperature-based comparison of compounds found in Bao Chong tea, green tea, and black tea** 14
Audrey Lin, Der-Lii Tzou, and Dino Ponnampalam
Kang Chiao International School, New Taipei City, Taiwan
- The effect of ultraviolet radiation and the antioxidant curcumin on the longevity, fertility, and physical structure of *Drosophila melanogaster*: Can we defend our DNA?** 21
Shan Lateef, Delaney Walts, and LaRina Clark
Benton Middle School, Manassas, VA
- The effect of caffeine on the regeneration of Brown Planaria (*Dugesia tigrina*)** 26
Olivia Lazorik and Michael Lazorik
Phillips Exeter Academy, Exeter, New Hampshire

All articles are copyright © 2019 to their respective authors. All JEI articles are distributed under the attribution non-commercial, no derivative license (<http://creativecommons.org/licenses/by-nc-nd/3.0/>). This means that anyone is free to share, copy and distribute an unaltered article for non-commercial purposes provided the original author and source is credited.

Measuring exoplanetary radii using transit photometry

Sarah Tang¹, William Waalkes²

¹Fairview High School, Boulder, Colorado

²University of Colorado, Boulder, Colorado

SUMMARY

The goal of this study was to measure the radii and constrain the orbital periods of three hot Jupiter exoplanets: HAT-P-25b, HAT-P-9b, and HAT-P-30b. Raw images of the host stars were acquired from the Apache Point Observatory in New Mexico. A data processing pipeline utilizing the Python programming language was used to convert the raw data images into calibrated pixels and transit light curve graphs. The graphs of HAT-P-25b and HAT-P-30b were fit with multiple light curve models, which varied based on a given range of radius and time of mid-transit parameters within the code. The data of HAT-P-9b were not further analyzed due to a non-detection in the data. We hypothesized that the differences between the dates the exoplanets were discovered and the dates on which we observed them have no effect on the radii of the exoplanets and their times of mid-transit. Chi-square Goodness of Fit tests were performed on all light curve models to isolate the chi-square value closest to 1.0. Chi-square maps were used to estimate the 1σ error bars for all light curve calculations. A significant shift in mid-transit time (-0.41 ± 0.31 hours from expected value) was detected for HAT-P-25, and a significant difference (0.04 ± 0.0020) from the literature value was calculated for the normalized radius (R_p/R_*) of HAT-P-30b. These findings stress the importance of updating exoplanetary measurements and will help scientists obtain more accurate knowledge about the characteristics of these exoplanets and their evolution over time.

INTRODUCTION

Exoplanets are planets that orbit a star other than the Sun (1). The study of exoplanets enables increased understanding about the formation of planets, interactions between planets, and how Earth's solar system differs from other solar systems (2).

Many detection methods exist to help discover these exoplanets; one such method is known as the transit detection method. Since planets orbit their host stars in consistent time frames, they can be detected through planetary transits, which occur when a planet crosses the disk of its host star. From the observer's viewpoint, the exoplanetary transit

causes a dimming in the detected amount of light emitted from the host star (3). This change in stellar flux is analyzed through the process of photometry (light measurement) to determine whether a planet is transiting or not. The transit detection method is the only exoplanet detection method that can measure the radius of the given exoplanet, making it a highly valuable and efficient approach (4).

Moreover, the recent development of new technologies and equipment has allowed for further exploration and discovery of exoplanets specifically using the transit detection method. A clear example of this advancement was the Kepler Mission, launched in 2009 by the National Aeronautics and Space Administration. This mission aimed to detect exoplanets specifically using the transit photometry method. By 2015, Kepler had detected 1030 exoplanets (5).

In this study, we analyzed the transit light curves of three exoplanets: HAT-P-25b, HAT-P-9b, and HAT-P-30b, to measure their radii and constrain their orbital periods to analyze if and how these planets have changed since their discovery. HAT-P-25b, HAT-P-9b, and HAT-P-30b are all hot Jupiter exoplanets, which are defined as gas giants with orbital periods of ten days or less. We hypothesized that the differences between the dates the exoplanets were discovered and the dates on which we observed them would have no effect on the radius and time of mid-transit parameters of the exoplanets. To test this hypothesis, we compared our calculated values to the previously published literature values for the radius and time of mid-transit parameters of each exoplanet observed: HAT-P-25b, HAT-P-9b, and HAT-P-30b (6-8). The literature values for each planet were obtained in 2010, 2009, and 2011, respectively (6-8).

The overarching goal of our research was to gain information regarding how exoplanets change over time and how these exoplanets compare to the planets within the Earth's solar system through the analysis of exoplanet characteristics. The results from this study would increase the understanding of planetary characteristics in general, and may provide information on how the parameters of planets in the Earth's solar system are projected to change in the near and far future. We focus on the radii and orbital periods of exoplanets because these measurements are used in many equations that calculate other planetary characteristics, such as mass and density. Furthermore, the study of exoplanets is a relatively new field, and limited follow-up analysis has been performed on the exoplanets already detected and confirmed.

Research regarding follow-up studies on exoplanets is critical for ensuring that we are obtaining accurate data regarding general planetary characteristics, so that in a larger sense, we can meticulously study planetary populations.

RESULTS
Light Curve Analysis

To study the transit light curve graphs of HAT-P-25b and HAT-P-30b in terms of relative light flux, the graphs were normalized to a baseline value of one. We were able to calculate the normalized radii of both planets using the following transit depth equation:

$$\text{Equation 1} \quad \frac{\Delta F}{F} = \frac{R_p^2}{R_\star^2}$$

where ΔF is the observed change in flux, F is the stellar flux, R_p is the radius of the planet, and R_\star is the radius of the star that hosts the planet.

Our results do not support our hypothesis because the values that we detected for the time of mid-transit of HAT-P-25b and the radius of HAT-P-30b (calculated to be 0.15 ± 0.02) differed from the literature values with statistical significance. For HAT-P-25b, we found the normalized radius to be 0.13 ± 0.03 , which is consistent with the literature value of 0.1275 ± 0.0024 (Table 1). However, the mid-transit time we found for HAT-P-25b was shifted -0.41 ± 0.31 hours from the expected value (Figure 1a). Our calculated mid-transit time significantly differs from the expected mid-transit time of 0 by more than the 1σ error bar value (Figure 2a). The 1σ error bar values for our light curve measurements were determined through chi-squared maps, which are visualizations of the 1σ error bar region of a measurement.

The expected mid-transit time is 0 because the best-fit model for our transit light curve is based on the orbital period stated in the literature (6). Basing our light curve model on this existing parameter, comparisons can be made between our measurements and the literature values, namely in regards to the mid-transit time of the exoplanet. This detected shift for HAT-P-25b indicates that the orbital period of this planet can be constrained further with future analysis.

For HAT-P-30b, the normalized planetary radius was calculated using equation 1 to be $0.15 \pm 0.02 R_p/R_\star$. This

Parameter	Calculated value	Literature value
Normalized planetary radius (R_p/R_\star)	0.13 ± 0.030	0.13 ± 0.002
Mid-transit time (hours from expected value)	-0.41 ± 0.310	
Orbital period (days)		3.65 ± 0.00002

Table 1. Measured results and the corresponding literature values for the normalized planetary radius (R_p/R_\star), time of expected mid-transit (hours), and orbital period (days) of HAT-P-25b.

value significantly differs from the literature result by a value of $0.04 \pm 0.0020 R_p/R_\star$ (Table 2) (8). This signifies that the radius of this planet can be constrained further. As for the time of mid-transit, we detected a value of 0.11 ± 0.20 hours from the expected time, and since the expected mid-transit time of 0 falls within the 1σ error bar values of our results, we can conclude that the period of this planet is robust and consistent (Figure 1c).

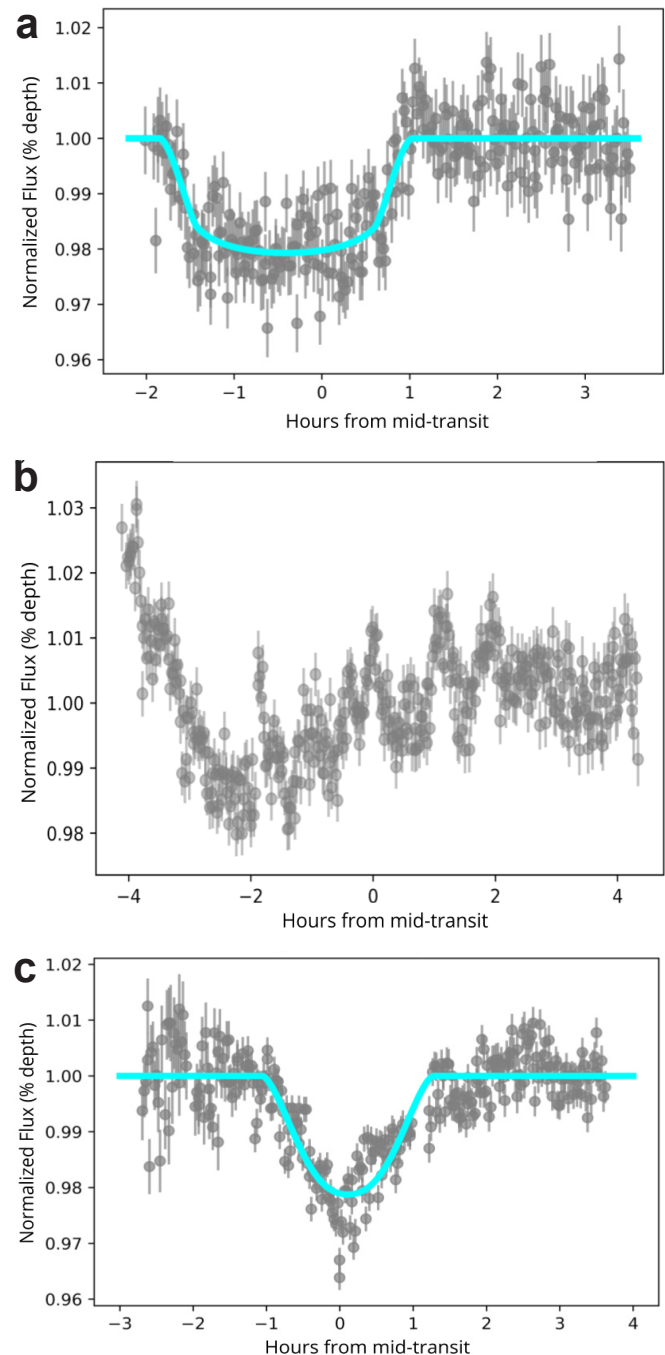


Figure 1. Normalized transit light curve graphs for the planets (a) HAT-P-25b, (b) HAT-P-9b, and (c) HAT-P-30b. These transit light curve graphs have been modeled with a best-fit transit light curve.

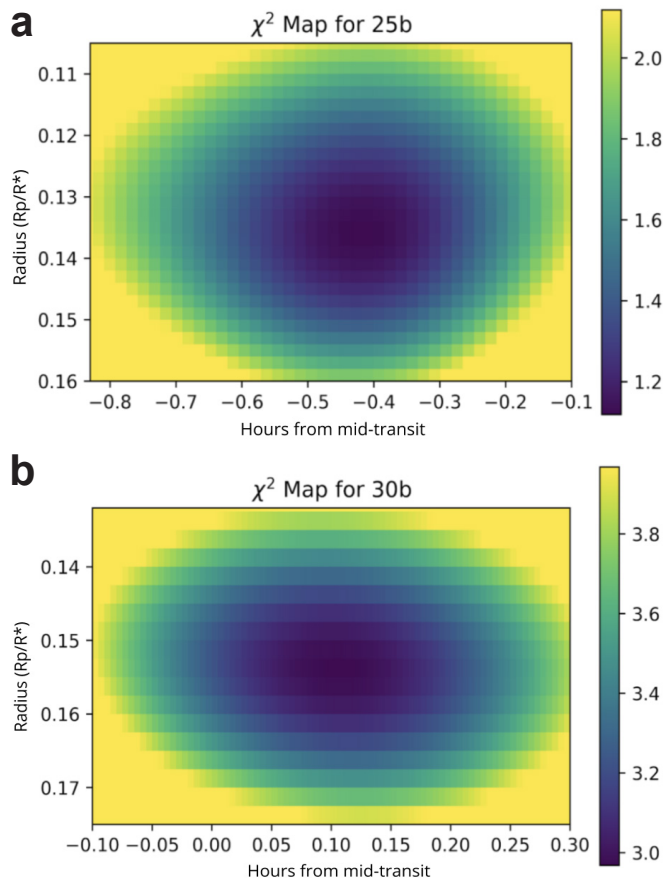


Figure 2. Chi-square maps for the calculated values of (a)HAT-P-25b and (b)HAT-P-30b. The 1σ error bar range is shown in purple, blue, and green.

DISCUSSION

In this study, we detected a significant shift from the literature value in the mid-transit time of the hot Jupiter exoplanet, HAT-P-25b (6). This information will be helpful to more accurately predict the transit times for this planet in the near future. HAT-P-25b was discovered in 2010, and since our plots are modeled on the parameters found at that time, our study signifies that the time of mid-transit has shifted by -0.41 hours in the past 8 years, and approximately 3.1 minutes every year. This means that the center of this transit occurred approximately 24 minutes earlier than expected.

It is important to keep information about planetary periods updated to actively study and keep track of these planets. The importance of this detected change in the time of mid-transit is demonstrated by the fact that in 20 years, HAT-P-25b will transit more than one hour earlier than the expected time. This is a substantial amount of time when observing planets.

Furthermore, the shift in the mid-transit time of HAT-P-25b implies that the orbital period of this exoplanet has shifted from $3.652836 \text{ days} \pm 0.000019 \text{ days}$, as stated in the literature, to around $3.653 \text{ days} \pm 0.017 \text{ days}$ (6). However, the actual constraint of the orbital period of HAT-P-25b cannot be determined until additional data is collected of a current span of continuous transits of HAT-P-25b.

Parameter	Calculated value	Literature value
Normalized planetary radius (R_p/R_*)	0.15 ± 0.020	0.11 ± 0.002
Mid-transit time (hours from expected value)	0.11 ± 0.200	
Orbital period (days)		2.81 ± 0.000005

Table 2. Measured results and the corresponding literature values for the normalized planetary radius (R_p/R_*), time of expected mid-transit (hours), and orbital period (days) of HAT-P-30b.

The significant difference that was detected for the normalized radius of HAT-P-30b ($0.04 \pm 0.0020 R_p/R_*$) can be used to more accurately constrain the radius of this planet for more precise measurements. No significant difference was found for the mid-transit time of this planet compared to literature results found in 2011 (8). This signifies that the orbital period of this planet is consistent and unfluctuating.

These detected differences may be the result of instrumentation factors or slight dissimilarities to the instrumentation techniques used by the mission that initially detected these exoplanets. Alternatively, these results may have occurred from the existence of true planetary characteristic changes, although this conclusion cannot be drawn until more data concerning these exoplanets are analyzed.

Since our hypothesis was not supported by our data, and statistically significant differences were found for the time of mid-transit of HAT-P-25b and the radius of HAT-P-30b, we can conclude that these characteristics can be constrained with further analysis. These results also stress the importance of updating exoplanetary characteristics' measurements for the accurate study of planetary populations and solar systems as a whole. Overall, these findings will encourage and allow scientists to obtain more accurate knowledge about these exoplanets and their characteristics.

METHODS

In the Kepler Mission, the Kepler Data Processing Pipeline was used to convert raw photos taken from a telescope and camera into calibrated pixels and transit graphs. The stages in the Kepler Pipeline include data acquisition, calibration, photometry, presearch data conditioning, transiting planet search, and data validation (9). In our study, we used a data processing pipeline with similar stages to the Kepler Pipeline: data acquisition, calibration, photometry, light curve modeling, and light curve analysis.

Data Acquisition

We used the 0.5 meter Astrophysical Research Consortium Small Aperture Telescope (ARCSAT) and Flare Camera imaging instrument located in Sunspot, New Mexico, during the nights of January 16, 17, and 18 of 2018 to collect the data. We used these instruments through remote observing on a computer. The three planets we observed (HAT-P-25b,

HAT-P-9b, and HAT-P-30b) are all hot Jupiter exoplanets, therefore, we used the R filter on the Flare Camera because these types of planets and their host stars tend to emit wavelengths of light between 550 and 800 nanometers (10-11). This filter was used to produce the most accurate images possible for the given target host stars.

Calibration

Using the ARCSAT telescope and the Flare Camera imaging instrument, we acquired four types of images: raw data science images, bias images, dark images, and domeflat images. The raw data science images were taken of the target star and neighboring comparison stars. Bias images are short exposures taken with the camera cover on to block out any light exposure. Dark images are bias images with shorter frame times, that specifically correct for the amount of accumulated electrons currently present on the Charge-Coupled Device (CCD) detector. Both dark and bias images reduce CCD flaws and increase signal-to-noise ratio of the data to obtain the highest amount of accuracy. Domeflat images are 60 second exposures taken of the inside of the observatory dome for consistency. These images reduce pixel sensitivity variations within the CCD (12).

Using these bias, dark, and domeflat images, we created the Masterbias, Masterdark, and Masterflat images. To create these Masterimages, all images of that specified image type were stacked and averaged using the Python programming language. Equation 2 was then used to obtain the final calibrated images:

$$\text{Equation 2} \quad \frac{(\text{Raw Science} - \text{MasterDark})}{(\text{Masterflat} - \text{Masterbias})}$$

These calculations were completed using the Python programming language.

Photometry

We used a graphical user interface titled AstrolmageJ to stack all of the final calibrated image files to perform aperture photometry (light measurement within a fixed size) on the target star and three neighboring comparison stars (13). These light measurements of the target and comparison stars were then normalized and converted into numerical values of light flux. These values of relative light flux for each image were stored in text files along with their corresponding 1σ error bar values (generated by AstrolmageJ) and barycentric Julian date, which is the time that the image was taken.

Light Curve Modeling

For each observed exoplanet, we used the timestamp and light flux value (as generated by AstrolmageJ) of the target star from each image to generate the transit light curve graphs of HAT-P-25b (**Figure 1a**), HAT-P-9b (**Figure 1b**), and HAT-P-30 (**Figure 1c**), with hours from mid-transit on the x-axis and normalized flux on the y-axis. These graphs were created through the Python programming language. Then, to

study the transit light curves in terms of relative light flux and transit depth, we fit a line to the baseline flux of the transit light curve graph and normalized that baseline value to a value of one.

However, the data collected for HAT-P-9b were not analyzed further because there is a non-detection in the data, which could be due to instrumentation or Charge-Coupled Device errors.

The BATMAN Python package was used to fit multiple light curve models to the HAT-P-25b and HAT-P-30b normalized transit light curve graphs (14). These models were varying based on a given range of values for the radius and time of mid-transit parameters within the code. Chi-squared goodness of fit tests were performed on each light curve model to find the chi-squared value closest to 1.0, which would signify a strong data to model fitting. We found the reduced chi-square values for HAT-P-25b and HAT-P-30b to be 1.1 (**Figure 2a**) and 2.9 (**Figure 2b**), respectively.

ACKNOWLEDGMENTS

We would like to thank Dr. Paul Strode (Department of Biology, Fairview High School) for providing guidance and support, and teaching me about the nature of science.

Received: November 28, 2018

Accepted: April 18, 2019

Published: May 7, 2019

REFERENCES

1. Fridlund, Malcolm, *et al.* "The way forward." *Astrophysical Journal*, vol. 205, no. 4, (2016): pp. 349-372., doi:10.1007/s11214-016-0247-2.
2. Carson, Joseph, *et al.* "Why Study Exoplanets?". College of Charleston, (2013): www.exoplanets.cofc.edu/why.html.
3. Clampin, M., *et al.* "Detection of Planetary Transits with the James Webb Space Telescope." *European Space Agency*, (2007): www.sci.esa.int/jwst/47523-clampin-m-et-al-2007/#.
4. Braun, Kaspar von, *et al.* "Searching for Planetary Transits in Galactic Open Clusters." *Astronomical Society of the Pacific*, vol. 117, no. 828, (2005): pp. 141-159., doi:10.1086/427982.
5. Soutter, Jack, *et al.* "The Kilodegree Extremely Little Telescope: Searching for Transiting Exoplanets in the Northern and Southern Sky." *Australian Space Research Conference*, (2015): www.researchgate.net/publication/302569516.
6. Quinn, S.N., *et al.* "HAT-P-25b: a Hot-Jupiter Transiting a Moderately Faint G Star." *The Astrophysical Journal*, vol. 745, no. 1, (2011): pp. 80-89., doi:10.1088/0004-637X/745/1/80.
7. Shporer, Avi, *et al.* "HAT-P-9b: A Low Density Planet Transiting a Moderately Faint F star." *The Astrophysical Journal*, vol. 690, no. 2, (2008): pp. 1393-1400., doi:10.1088/0004-637X/690/2/1393.

8. Johnson, John Asher, et al. "HAT-P-30b: A Transiting Hot Jupiter on a highly oblique orbit." *The Astrophysical Journal*, vol. 735, no. 1, (2011): pp. 24-31., doi:10.1088/0004-637X/735/1/24.
9. Tenenbaum, Peter, et al. "Detection of Transiting Planet Candidates in Kepler Mission Data." *National Aeronautics and Space Administration*, (2012): www-conf.slac.stanford.edu/statisticalissues2012.
10. Wang, Ji, et al. "On the Occurrence Rate of Hot Jupiters in Different Stellar Environments." *The Astrophysical Journal*, vol. 799, no. 2, (2009): pp. 229-237., doi:10.1088/0004-637X/799/2/229.
11. Hawley, Suzanne, et al. "ARCSAT." New Mexico State University, (2014): www.apo.nmsu.edu/Telescopes/ARCSAT/index.html.
12. "The Types of Images." *Raw Astrophotography Data*, www.rawastrodata.com/pages/typesofimages.html.
13. Collins, Karen A., et al. "AstroImageJ: Image Processing and Photometric Extraction for Ultra-Precise Astronomical Light Curves (Expanded Edition)." *AstroImageJ: ImageJ for Astronomy*, (2017): www.astro.louisville.edu/software/astroimagej.
14. Kreidberg, Laura. "batman: BAsic Transit Model cAlculationN in Python." *Publications of the Astronomical Society of the Pacific*, vol. 127, (2015): pp. 1161-1165., www.cfa.harvard.edu/~lkreidberg/batman.

Copyright: © 2019 Tang and Waalkes. All JEI articles are distributed under the attribution non-commercial, no derivative license (<http://creativecommons.org/licenses/by-nc-nd/3.0/>). This means that anyone is free to share, copy and distribute an unaltered article for non-commercial purposes provided the original author and source is credited.

Financial Support: Thanks to JEI Sponsor Alloy Therapeutics for support of this article's publication.

An analysis of soil microhabitats in Revolutionary War, Civil War, and modern graveyards on Long Island, NY

Dominick Caputo¹, Jason Rattansingh¹, Victoria Hernandez¹, and Bruce Nash²

¹ William Floyd High School, Long Island, NY

² Cold Spring Harbor Laboratory, Long Island, NY

SUMMARY

Previously established data indicate that cemeteries have contributed to groundwater and soil pollution. This study aimed to determine whether there was a variation in the microbes in cemeteries due to embalming techniques and to identify primary microbial communities in each cemetery. Different embalming techniques were used during different eras in recent history. These fluids can impact both epinecrotic and thanatomicrobiomes, the microbiomes that exist in decomposing remains. Additionally, these fluids can seep into the microbial communities, affecting the microbiome composition, and continue to leach into the larger surrounding environment, contributing to water source and aquifer pollution. We evaluated the 16S rDNA microbial gene followed by QIIME analyses using the Jupyter Notebooks application. We hypothesized that microbial variation would be high between cemeteries of different eras due to dissimilarities between embalming techniques employed, and furthermore, that specific microbes would act as an indication for certain contaminants. The results indicate that the following phyla were present: Proteobacteria, Planctomycetes, Bacteroidetes, Actinobacteria, Chloroflexi, Verrucomicrobia, Acidobacteria, and AD3. These taxonomic classifications were present in all sites with the exception of AD3 which was absent in the Civil War Cemetery. Overall, cemetery sites were clustered together based on location due to variations in the concentrations of the phyla and their more specific taxa.

Introduction

A microbiome is a collection of microorganisms that reside in a particular environment, and microbiomes are the basis for all ecosystems. Microorganisms are partially responsible for the intake of carbon into an organism, as well as contributing to tissue growth or the decomposition and recycling of biomatter (1). The biodiversity within microbiomes is important to study because it can indicate the health of an environment and whether or not pollution is present (2). Microbiomes can metabolize or respond to many different chemicals, and different microbes can succeed in different environments due to their metabolisms. Additionally, microorganisms are responsible for carbon uptake, oxygen release, and nitrogen conversion (3).

Cemeteries contain unique microbiomes that require special attention due to the risks of soil or water contamination (4). The type of embalming fluids used may contribute to pollutants in aquifers. Revolutionary War cemeteries used no embalming techniques, Civil War cemeteries used arsenic, and modern cemeteries use formaldehyde (5). Approximately 827,060 gallons of embalming fluid is also buried, which primarily consists of formaldehyde (6).

Leachate is water that has percolated through the soil and retains some of the pollutants within the soil. Leachate can contribute to the spreading of harmful substances such as the components of embalming fluids. If not properly contained, leachate can have noticeable implications to the surrounding ecosystem health, as contaminated leachate may contain pathogenic bacteria and viruses that can contaminate drinking water (4).

Certain microbes have been identified as able to metabolize either arsenic or formaldehyde, which are used by these microbes to perform functions such as anaerobic respiration, methylation, detoxification, and assimilation (7). Previous research suggests the possibility for heavy metal contamination from embalming fluids at gravesite locations. Copper, lead, zinc, and iron have been found in increased concentrations at gravesites as well as a dramatic increase, as opposed to cemeteries not using embalming fluids, in arsenic levels indicating graveyard contaminates (8). Heavy metal pollution from sources such as iron, copper, and zinc has been shown to have carcinogenic and non-carcinogenic negative health implications, especially for children and people living on or near contaminated areas (9).

Three cemeteries were selected in Long Island, NY in this study based on the time period when burials were taking place. The Manor of St. George, New York contains a cemetery that houses bodies from 1775-1783, the Revolutionary War era. The Union Cemetery in Middle Island contains bodies from 1861-1865, the Civil War era. The Holy Sepulcher Cemetery in Coram contains bodies which have been buried in the past 50 years, roughly.

The purpose of the study is to determine if the different burial techniques utilized have affected the surrounding areas' soil microbiomes. We hypothesized that there will be a high variation in microbiomes between the three cemeteries, due to the dissimilarities in embalming techniques. Triplicate samples were collected from three different cemeteries and the 16S gene was isolated and amplified. The samples were

then sequenced and processed through a data informatics pipeline to create graphical representations of the data. There was variation between all three locations; however, the distance was the greatest between the Civil War cemetery relative to the other two cemeteries.

Results

Phyla Present Across All Cemeteries

To reiterate, this research was conducted in order to determine if there were varying concentrations of microbiomes, due to dissimilarities in embalming technique. This research was conducted by analyzing the 16S rRNA gene which yields data on microbial taxonomic presence and approximate population counts. Post sequencing, the data was analyzed through a bioinformatics pipeline (QIIME) and generated graphical representations of microbial data.

Each sample taken from the various cemeteries contained similar phyla. The predominant phyla present included: Proteobacteria, Planctomycetes, Bacteroidetes, Actinobacteria, Chloroflexi, Verrucomicrobia, Acidobacteria. The phylum AD3 is present in both the modern and Revolutionary cemeteries but appears to be absent within the Civil War cemeteries (**Figures 1 and 2**).

Alpha Diversity Between the Soil of Different Cemeteries

Alpha diversity is a measure of microbial diversity within a specific location, which indicate species richness. Again, the aims of this project were to determine if microbiomes varied due to different embalming techniques. The sediments of the Civil War cemetery appear to have the highest microbial species richness while the Revolutionary War cemetery contains the lowest (**Figure 3**).

Variations Between the Civil War, Modern, and Revolutionary War Cemeteries

The Civil War cemetery contained many phyla that are similar to the other cemeteries but are present in different concentrations (**Figure 1**). The Civil War site contained more taxa that appeared to be evenly distributed (**Figure 3 and 5**). The Principal Component Analysis (PCoA) demonstrated the increased variation between the microbial Civil War community in comparison to the Revolutionary War and

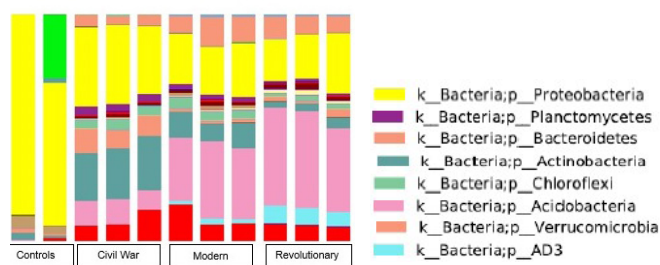


Figure 1. Phyla concentrations in different cemeteries. Shown above is a taxonomic plot that represents the phyla concentrations in different cemeteries. Most notably, AD3 was present in all sites, with the exception of the Civil War cemetery.

modern cemeteries (**Figure 4**). This indicates that there are differences in the microbial communities, with the Civil War cemetery demonstrating the largest difference as compared to the other two sites.

The Civil War cemetery contained greater Proteobacteria concentrations, which varied from 29% – 35% (**Figure 1**). In contrast, the other cemetery samples had lower representations with the highest being 26% and the lowest being 18%. Another aspect contributing to this variation in beta diversity, is the Civil War cemetery consisted of greater Bacteroidetes proportions, averaging 9.22% in contrast to modern Cemeteries, which contained approximately 2.16% and Revolutionary which contained 1.38% relative amount, which would heavily impact species richness. The two phyla in which the Civil War cemetery contained lower representations were: Acidobacteria and Verrucomicrobia. The Civil War Cemetery contained the least Acidobacteria representation, averaging 10.26% compared to modern Cemeteries which is shown to have approximately 40.91% and Revolutionary which contained 23.56% Acidobacteria representation. The Civil War cemetery contained the lowest Verrucomicrobia representation, averaging 4.36% as opposed to modern cemeteries which contained approximately 8.23%, and Revolutionary cemeteries, which contained 10.46% Verrucomicrobia representation.

Discussion

The research question posed was: Is there a variation in microbiomes in Revolutionary, Civil War, and modern cemeteries? It was hypothesized that microbial variation would be high between different era cemeteries due to dissimilarities between embalming techniques employed. The data indicates the microbial communities within each of the cemeteries are clearly distinct but consist of many of the same bacterial phyla. Phyla such as Proteobacteria, Planctomycetes, Bacteroidetes, Actinobacteria, Chloroflexi, Verrucomicrobia, and Acidobacteria were present across all

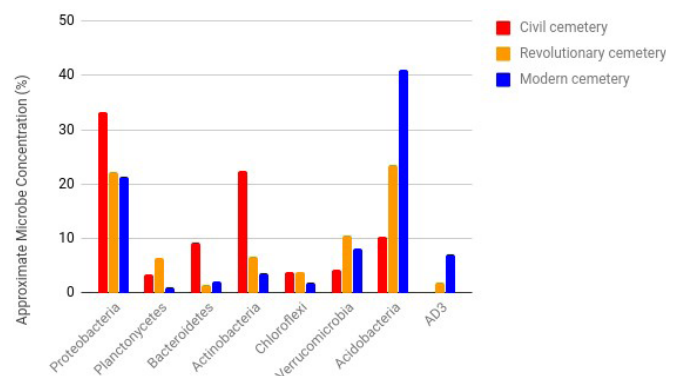


Figure 2. Microbe concentrations in different cemeteries. Results from the bar graph further support the lack of AD3 within the Civil War Cemetery. Additionally, of the primary phyla present, Proteobacteria, Bacteroidetes, and Actinobacteria are at notably higher concentrations at the Civil War site.

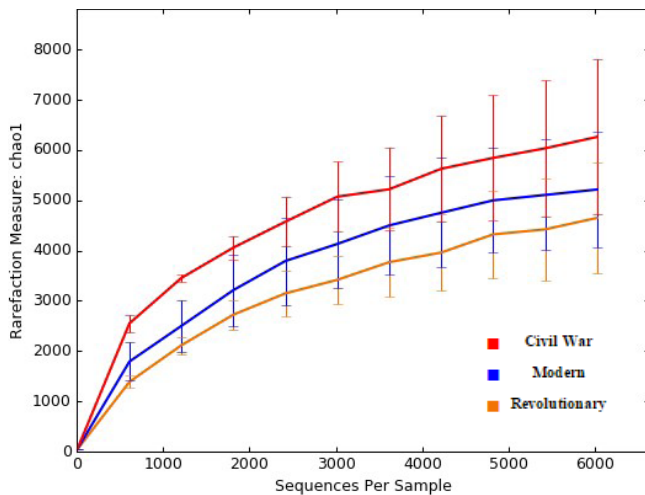


Figure 3. Microbial species richness of sediments from different era cemeteries. The rarefaction chart data indicates that the Civil War cemetery had the highest alpha diversity while the Revolutionary War contained the lowest.

locations (Figures 1 and 2). Proteobacteria and Acidobacteria are a diverse set of heterotrophic microorganisms that are expected to reside within soil microbial communities. Previous research indicates that cultured Acidobacteria are capable of utilizing carbohydrates, fixing nitrites, and can respond to both macronutrients and micronutrients within acidic soil (10). Additionally, Verrucomicrobia and α -Proteobacteria are associated with the soil microbial communities near forested regions (11). The only phyla that was highest in the Revolutionary War cemetery was Verrucomicrobia (Figure 2). This is relevant as this cemetery was more heavily wooded than the other two sites. The Revolutionary site also had the highest concentration of Planctomycetes. This phylum is metabolically diverse but is capable of sulfur and sulfide reduction in both aerobic and anaerobic conditions (12). Throughout all sample sites, the Revolutionary War site had the lowest concentrations of Chloroflexi, a phylum that is strongly associated with the metabolism in ecosystems containing high nitrogen and organic matter concentrations (13). This may indicate that the Revolutionary War site contained the lowest concentrations of organic decaying matter.

The rarefaction plot in suggests that the Civil War cemetery had the highest microbial species richness while the Revolutionary War cemetery contained the lowest (Figure 3). This may be attributed to the variations between microbial presence between the different sites.

Each community is clearly clustered together based on location, as seen in the PCoA plot (Figure 4). Out of the sites analyzed, the most distinct microbiome was found at the site containing bodies from the Civil War time period. This was evident as it had the highest distance in relation to the other sample sites (Figure 4). For example, although Proteobacteria, Bacteroidetes, and Actinobacteria were present in all sites, they are present in notably higher concentrations at the Civil

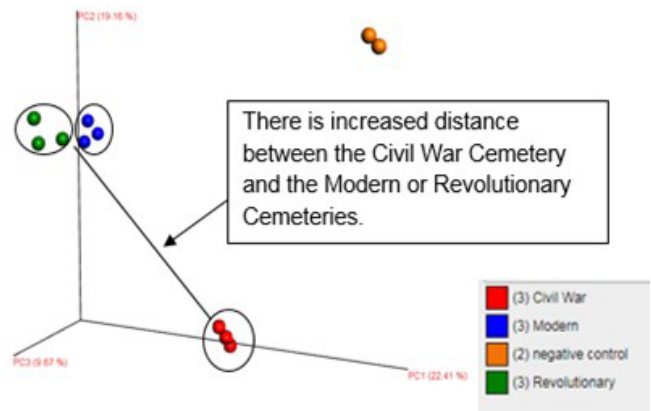


Figure 4. Principle component clusters of microbes from Revolutionary, Civil War, and Modern eras. The large distance between the three sample sites on the principle component analysis (PCoA) plot is indicative of high beta diversity between the Civil War microbial community and the other two cemeteries. The modern and Revolutionary War cemeteries are clustered more closely together suggesting similarities between microbes present in those two communities while still maintaining distinct microbiomes. Additionally, it is important to note that the lab controls are distinctly separate from all samples, supporting the validity of the results.

War site (Figure 2). Additionally, this site also contained the highest species richness (Figure 3). These distinctions may be attributed to numerous abiotic and biotic factors including but not limited to: soil pH, biomatter presence, different rates of decaying bodies, embalming techniques, and different ecosystems in close proximity to the cemeteries (14).

High concentrations of Koribacteraceae and Ellin 6513 bacteria are present within the modern and Civil War cemeteries and are decreased or negligible within the Revolutionary War cemetery. This may be attributed to decomposing biomatter present in modern and Civil War

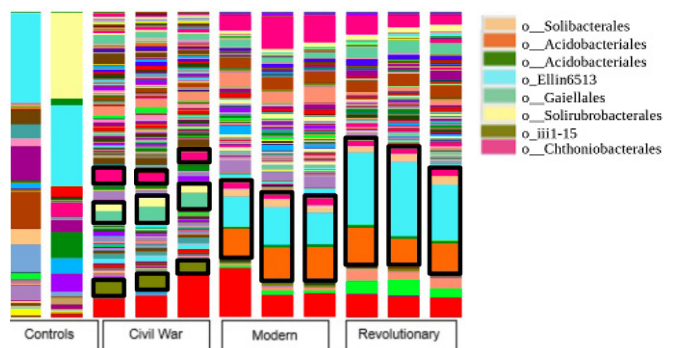


Figure 5. Distribution of taxa. The taxonomic plot depicts the microbial orders and distribution of taxa present. Bolded boxes highlight the orders on the legend to the right. This depicts that the Civil War era cemetery has a microbiome that is greatly different than the other two. The iii1-15 microbes were somewhat successful in the Civil War era cemetery while present in near negligible amounts in the Modern and Revolutionary War cemeteries. The Ellin6513 microbes are the opposite of iii1-15, where they are successful in the Modern and Revolutionary war era cemeteries while present in small amounts in the Civil war era cemeteries.

cemeteries, but not necessarily present in Revolutionary War cemeteries due to increased time elapsed for bodies to decompose (15). Another variation evident between communities was that increased Acidobacteria was present in the Revolutionary War cemetery (Figure 2). This is indicative of low soil pH; however, that cannot be confirmed (14).

The PCoA plot also demonstrates that the distance was the least between the Revolutionary War cemetery and the modern cemetery (Figure 4). They also had similar microbe concentrations (Figure 2) and were closer in species richness (Figure 3). This may be attributed to caskets used in modern cemeteries and increased decomposition of bodies present in the Revolutionary War cemetery. Conversely, the Civil War cemetery was the furthest from the other sample sites on the PCoA plot (Figure 4). This variation may be due to the lack of the AD3 or containing sediment that can support high species richness (Figures 2 and 3). This could also be due to consisting of notably higher concentrations of Proteobacteria, Bacteroidetes, and Actinobacteria or, containing notably lower concentrations of Verrucomicrobia and Acidobacteria (Figures 1 and 2). It could also be due to different abiotic and biotic factors influencing microbial diversity.

Overall, according to the data presented, there is a variation in the microbiomes of the different eras' cemeteries. Data indicates the following: Proteobacteria, Bacteroidetes and, Actinobacteria concentration is increased in the Civil War cemetery. Verrucomicrobia and Planctomycetes concentration is increased in the Revolutionary War cemetery. While AD3 is only present in increased concentration in the modern cemetery, and Chloroflexi is present in decreased concentration in the modern cemetery. These variations are believed to be due to a number of factors such as pH level, biomatter variation, caskets utilized, and dissimilarities in burial techniques.

Materials and Methods

At each graveyard, samples were collected 12 inches beneath the organic layer in a corner that is not directly above a gravesite. At each sample site, approximately 2.0 grams of soil was collected in triplicate. The 2014 Detailed MO BIO protocol (Powersoil DNA isolation kit, Qiagen) was used for DNA extraction and isolation (16). 0.25 grams of soil was added into MO BIO PowerBead Tubes alongside negative controls, which were comprised of empty microfuge tubes. Following this, the tubes were mixed using a vortex. Then, 60 µl of Solution C1, a type of cell membrane lysis solution, was added. Afterwards, the tubes were vortexed to mix the contents. The tubes were mixed for 10 minutes using the vortex at maximum speed. The tubes were then centrifuged at 10,000 x g for 30 seconds at room temperature (16).

Then, 250 µl of Solution C2, a solution that aids in the precipitation of non-DNA organic and inorganic material such as humic substances, cell debris, and proteins, was added and the tubes were centrifuged again for 5 seconds, then incubated at 4°C for 5 minutes. After incubation, the tubes

were centrifuged again for 1 minute at 10,000 x g. Then, avoiding the pellet, 600 µl of the supernatant was transferred to a clean tube (16).

Then, 200 µl of Solution C3, another solution that aids in the precipitation of non-DNA material, was added, vortexed briefly, and incubated at 4°C for 5 minutes. The tubes were then centrifuged for 1 minute at 10,000 x g, and 750 µl of the supernatant was transferred to a clean tube. The solution was mixed before adding 1.2 ml of the Solution C4, a high-concentration salt solution, to the supernatant and vortexed for 5 minutes. Then, 675 µl of supernatant was loaded onto a spin filter and centrifuged at 10,000 x g for 1 minute at room temperature. The flow-through was discarded, and an additional 675 µl of supernatant was added to the spin filter and centrifuged at 10,000 x g for 1 minute at room temperature. The flow-through was discarded, and the remaining supernatant was loaded and centrifuged at 10,000 x g for 1 minute at room temperature (16).

Next, 500 µl of Solution C5, an ethanol-based wash solution used to further clean the DNA, was added and centrifuged at room temperature for 30 seconds at 10,000 x g. The flow-through was discarded from the 2ml Collection Tube. The remainder was centrifuged at room temperature for 1 minute at 10,000 x g. The spin filter was placed into a clean 2ml Collection Tube (16).

Then, 100 µl of Solution C6, an elution buffer, was added to the center of the white filter membrane. Then the tube was centrifuged for 30 seconds at 10,000 x g at room temperature. The spin filter was discarded. The DNA in the tube was then ready for further downstream applications (16).

After DNA extraction, the 16S gene was amplified using the 16S primer and a thermocycler. Gel electrophoresis was used in order to confirm that the 16S gene was amplified. The samples that successfully amplified were sent to Cold Spring Harbor Laboratory for indexing, and from there, to be sequenced using Illumina's MiSeq system. The resulting collection of sequences from each sample were analyzed using Quantitative Insights Into Microbial Ecology (QIIME) analyses conducted through the Jupyter Notebook web application, which allowed for the generation of the PCoA, rarefaction, and taxonomy plots.

Received: April 11, 2018

Accepted: October 29, 2019

Published: May 5, 2019

References

1. Todar, Kenneth, and Madison. *Impact of Microbes on the Environment*, textbookofbacteriology.net/Impact.html.
2. Ashbolt, Nicholas, et al. "13 Indicators of Microbial Water Quality." *Water Quality: Guidelines, Standards and Health*, 2001, pp. 289–316.
3. Bassil, Najj M., Nicholas Bryan, and Jonathan R. Lloyd. "Microbial degradation of isosaccharinic acid at high pH." *The ISME Journal* 9.2 (2015): 310.

4. Żychowski, J, and T Bryndal. "Impact of Cemeteries on Groundwater Contamination by Bacteria and Viruses - a Review." *Current Neurology and Neuroscience Reports.*, U.S. National Library of Medicine, June 2015, www.ncbi.nlm.nih.gov/pubmed/26042963.
5. Brenner, Erich. «Human body preservation—old and new techniques.» *Journal of anatomy* 224.3 (2014): 316-344.
6. Harker, and Alexandra. "Landscapes of the Dead: An Argument for Conservation Burial." *Berkeley Planning Journal*, 1 Feb. 2012, escholarship.org/uc/item/7br0d6c3.
7. Stolz, John F, *et al.* "Arsenic and Selenium in Microbial Metabolism." *Annual Reviews*, 8 May 2006, www.annualreviews.org/doi/abs/10.1146/annurev.micro.60.080805.142053.
8. Spongberg, A. L., & Becks, P. M. (2000, January). Inorganic Soil Contamination from Cemetery Leachate. Retrieved June 11, 2018, from <https://link.springer.com/article/10.1023/A:1005186919370>
9. Kielak, Anna M, *et al.* "A Review of Soil Heavy Metal Pollution from Mines in China: Pollution and Health Risk Assessment." *NeuroImage*, Academic Press, 25 Sept. 2013, www.sciencedirect.com/science/article/pii/S0048969713010176#.
10. Kielak, Anna M *et al.* "The Ecology of Acidobacteria: Moving beyond Genes and Genomes" *Frontiers in microbiology* vol. 7 744. 31 May. 2016, doi:10.3389/fmicb.2016.00744
11. Hackl, Evelyn *et al.* "Comparison of diversities and compositions of bacterial populations inhabiting natural forest soils" *Applied and environmental microbiology* vol. 70,9 (2004): 5057-65.
12. Elshahed, Mostafa S *et al.* "Phylogenetic and metabolic diversity of Planctomycetes from anaerobic, sulfide- and sulfur-rich Zodletone Spring, Oklahoma" *Applied and environmental microbiology* vol. 73,15 (2007): 4707-16.
13. Denef, Vincent J *et al.* "Chloroflexi CL500-11 Populations That Predominate Deep-Lake Hypolimnion Bacterioplankton Rely on Nitrogen-Rich Dissolved Organic Matter Metabolism and C1 Compound Oxidation" *Applied and environmental microbiology* vol. 82,5 1423-32. 19 Feb. 2016, doi:10.1128/AEM.03014-15.
14. Sait, Michelle, *et al.* "Effect of PH on Isolation and Distribution of Members of Subdivision 1 of the Phylum Acidobacteria Occurring in Soil." *Applied and Environmental Microbiology*, American Society for Microbiology, 1 Mar. 2006, aem.asm.org/content/72/3/1852.short.
15. Dey, Uttiya *et al.* "Isolation and characterization of arsenic-resistant bacteria and possible application in bioremediation" *Biotechnology reports (Amsterdam, Netherlands)* vol. 10 1-7. 15 Feb. 2016, doi:10.1016/j.btre.2016.02.002
16. MO BIO Laboratories, Inc. (2014). *Manual* [PDF].
17. Javan, Gulnaz T, *et al.* "The Thanatobiome: A Missing Piece of the Microbial Puzzle of Death" *Frontiers in microbiology* vol. 7 225. 24 Feb. 2016, doi:10.3389/fmicb.2016.00225

Copyright: © 2019 Caputo *et al.* All JEI articles are distributed under the attribution non-commercial, no derivative license (<http://creativecommons.org/licenses/by-nc-nd/3.0/>). This means that anyone is free to share, copy and distribute an unaltered article for non-commercial purposes provided the original author and source is credited.

Financial Support: Thanks to JEI Sponsor Alloy Therapeutics for support of this article's publication.

A temperature-based comparison of compounds found in Bao Chong tea, green tea, and black tea

Audrey Lin¹, Der-Lii Tzou², Dino Ponnampalam¹

¹Kang Chiao International School

²Institute of Chemistry, Academia Sinica

SUMMARY

Tea is a widely-consumed beverage, and different types of tea can be produced depending on their oxidation levels. However, how different types of tea and brewing water temperature can affect health has not been considered. This investigation studied how compounds in tea such as caffeine, catechins, and L-theanine, were different in green tea, Bao Chong tea, and black tea, as well as in Bao Chong tea brewed with different water temperatures (25°C, 45°C, 75°C, 90°C) using NMR analysis. The results showed that Bao Chong Tea had the highest caffeine, catechins, and L-theanine content, followed by green tea and then black tea. The best temperature for brewing tea to produce caffeine, catechins and L-theanine was between 45°C and 75°C, and all chemical contents were reduced greatly at 90°C. A better understanding of the relationship between tea and its chemical contents will allow people to have better knowledge of their food intake, and possibly allow people to choose accordingly.

INTRODUCTION

The ability of a small green leaf to weave itself into cultures and societies throughout history is remarkable. From Imperial China to Victorian Britain, from Emperors to builders, tea is a rich, complex beverage that has affected numerous decisions and people. Since tea is a healthy and popular drink, this research aims to investigate tea. As people care more about their health, the benefits of tea have been more widely explored. People no longer only drink hot tea; cold tea has become a trending beverage as well [1]. However, the impacts of drinking various teas brewed in different temperatures remain uncertain.

Tea, the common name for *Camellia sinensis*, contains thousands of chemical compounds. Different compounds are released depending on how the tea is processed and brewed [2]. To make different types of tea that people like to drink, tea leaves are subjected to distinct processes [3]. The most known types of tea are: green tea, Bao Chong tea, and black tea. All tea starts off as *Camellia sinensis* leaves but are then distinguished further based on different levels of oxidation and processing [3]. Tea leaves are first harvested and withered, reducing the water content and allowing the antioxidants to develop and amino acids to degrade [4]. Maceration is then performed to allow oxidation by the physical

release of oxidative enzymes [3,4]. Oxidation is the natural chemical reaction by which new compounds are unlocked. The tea leaves begin to turn brown and new flavors are generated through biochemical modifications within the leaves [3]. When the desired oxidation process is over, fixation and drying are performed to reduce the activity of oxidative enzymes. Green tea is un-oxidized, black tea is fully-oxidized, and Bao Chong tea is semi-oxidized [2].

Out of the thousands of compounds found in tea, caffeine, catechins, and L-theanine are the most well-known ones [2]. Caffeine is popularly known for its ability to increase alertness and to keep people awake (Figure 1A). Catechins are famous for their antiviral properties, which can, for example, interfere with the replication cycle of DNA viruses and keep people healthier (Figure 1C) [5]. L-theanine is recognized for its anxiety-relieving effects as it increases dopamine levels and increases the production of alpha waves, which makes people more relaxed (Figure 1B) [6,7].

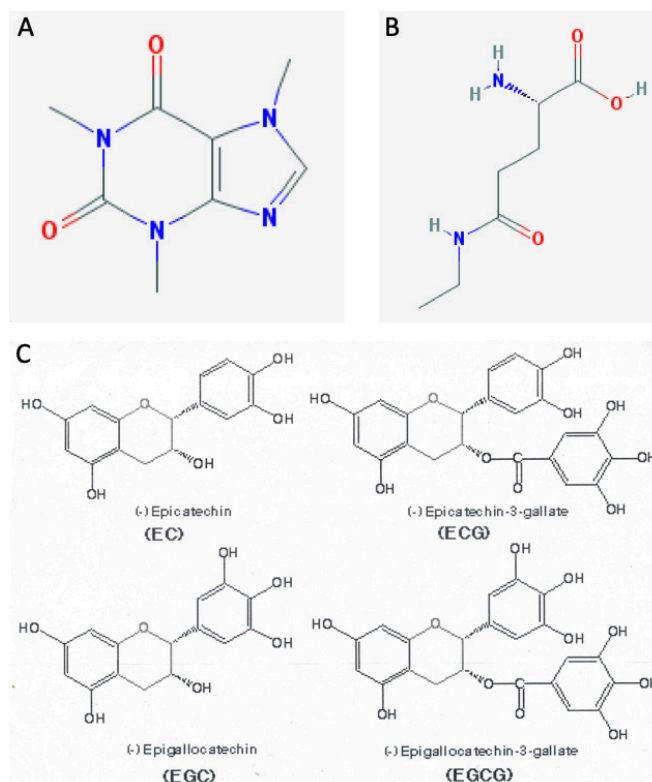


Figure 1. Chemical structures compounds found in tea. A. Chemical structure of caffeine (8). B. Chemical structure of L-theanine (10). C. Chemical structure of catechins (9).

It is important to study the relationship between tea contents and the types of tea because tea is a widely consumed beverage, and a better understanding of its composition will allow people to choose their preferences accordingly. Also, a better understanding of chemical contents in tea could lead to more developed applications in health. For example, green tea is suggested to be beneficial in reducing the risk for cardiovascular diseases [11]. Therefore, this research aims to gain a better understanding of how green tea, Bao Chong tea, and black tea can affect health, and how brewing temperature can affect the release of caffeine, catechins, and L-theanine. This research investigated how caffeine, catechins, and L-theanine are different in green tea, Bao Chong tea, and black tea and how water temperature affects the levels of caffeine, catechins, and L-theanine in Bao Chong tea. It was hypothesized that the levels of caffeine, catechins, and L-theanine in Bao Chong tea would be in between the levels found in non-oxidized green tea and fully-oxidized black tea because it is semi-oxidized. It was also hypothesized that higher water temperatures used to brew tea would result in higher concentrations of caffeine, catechins, and L-theanine because the high water temperature causes the breakdown of cell walls and the release of compounds.

RESULTS

Comparing caffeine, catechins and L-theanine in green tea, Bao Chong tea, and black tea

Three types of tea samples, green tea, Bao Chong tea and black tea, were brewed with 75°C water for three minutes and analyzed using NMR to compare the levels of caffeine, catechins, and L-theanine in tea. This experiment was conducted to test the hypothesis that semi-oxidized tea produces levels of tea compounds between non-oxidized and fully-oxidized tea.

The peaks are the highest in Bao Chong tea than in green tea and black tea. Bao Chong tea contained the most caffeine, catechin, and L-theanine content, followed by green tea and then black tea (Figure 2).

Comparing Bao Chong tea under 45°, 75°, and 90°C brewing water

Bao Chong tea samples were brewed in 45°C, 75°C, and 90°C water for three minutes. The supernatant liquid was extracted and analyzed using NMR to answer the research question of this investigation “How does water temperature affect the levels of caffeine, catechins, and L-theanine in green tea, Bao Chong tea, and black tea?”

The experiment showed that lower water temperatures resulted in higher chemical content (Figure 3). Both catechins and L-theanine content decreased as the brewing water temperature increased. The caffeine content remained about the same for 45°C and 75°C, then decreased for 90°C. Both caffeine and catechins peaks shifted upfield for 45°C and 75°C. There was also an unordered shifting pattern of caffeine peak in 7.60 ppm.

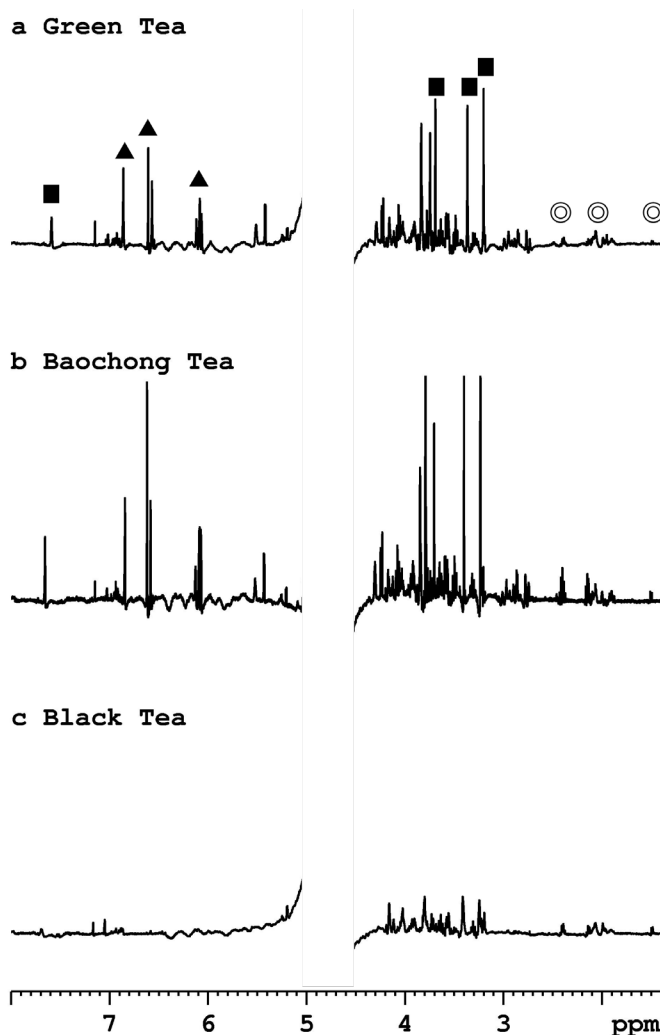


Figure 2. NMR analysis of the three tea samples. The spectra have been modified for easier reading. Corresponding peaks are denoted by ■ [caffeine]; ▲ [catechins]; circle [L-theanine]. Caffeine, catechins, and L-theanine are labeled according to the literature [12].

Through this experiment, it was found that levels of all three compounds tested: caffeine, catechins and L-theanine, remained the same for 45°C and 75°C, then decreased for 90°C (Table 1).

Comparing Bao Chong tea under 25° and 45°C brewing water

Bao Chong tea samples that were brewed under 25°C and 45°C were also analyzed using NMR. The 25°C trial used tea

	25°C	45°C	75°C	90°C
Brewing Time	12 hrs	3 mins	3 mins	3 mins
Caffeine	4:4:4:1	5:5:4:1	5:5:4:1	4:4:4:1
Catechin	1:4:1	1:3:1	1:3:1	1:2:1
L-theanine	4:1:1	4:1:1	4:1:1	2:1:1

Table 1. Ratio of Caffeine, Catechins, and L-theanine content integrated peaks. Each number represents a different peak.

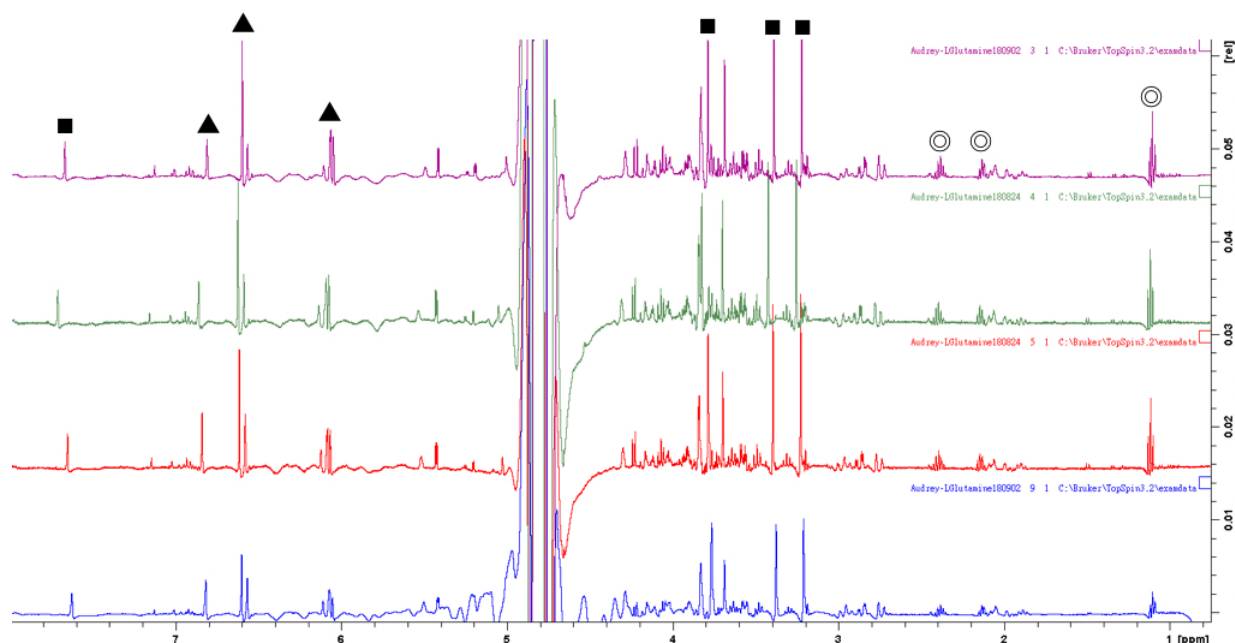


Figure 3. NMR Spectra of Bao Chong tea brewed in different temperatures of water. Tea was brewed at 25°C for 12hrs (purple), 45°C for 3 mins (green), 75°C for 3 mins (red), and 90°C for 3 mins (blue). Corresponding peaks are denoted by ■ [caffeine], ▲ [catechins], and circle [L-theanine].

leaves and was immersed for 12 hours, while the 45°C trial used tea leaf powder and was brewed for only 3 minutes. The different conditions were designed to match how people typically make cold tea, so the sample will be in a condition similar to when it is normally consumed [13]. This expands the brewing water temperature range and compares the two samples in a more applicable condition.

In this experiment, it was found that the amount of caffeine increased, catechins decreased, and L-theanine remained the same from 25°C to 45°C (Figure 4-6). However, there is a suspected structural change to either caffeine or a type of catechin (Figure 5,6). It was also found that the Caffeine and catechins peaks shifted upfield for about 0.01 ppm, and the peaks remain about the same in L-theanine (Figure 5,6). Besides the shifts, there was also a peak structural change at 3.8 ppm (Figure 5). The implications of the results are further clarified in the discussion section.

DISCUSSION

Comparing caffeine, catechins and L-theanine in green tea, bao chong tea, and black tea

A better understanding of the amounts of caffeine, catechins and L-theanine in different types of tea will allow people to choose their preferred type of beverage. For example, elders might want to consume less caffeine to prevent sleep disturbance [14]. The signals of the studied compounds are clearly detected: L-theanine within 1 to 2 ppm, caffeine within 3 to 4 and 7 to 8 ppm, and catechins within 6 to 7 ppm (parts per million) (Figure 2). Bao Chong tea had the highest caffeine, catechin, and L-theanine content, followed by green tea

and then by black tea (Figure 2).

However, the findings are not supported by existing literature. From the literature review, many studies suggested that green tea, which is un-oxidized tea, has the highest content of catechins and L-theanine, while black tea, which is the fully-oxidized tea, has the highest caffeine content [1,15,16]. The literature also suggests that half-oxidized tea has the highest caffeine content [17]. The outcome of this study, however, suggests that Bao Chong tea is the richest in all three compounds. A possible explanation of the differences could be the different production process or tea leaves used. Therefore, various tea brands or origins could be compared in future studies.

For all three tea samples, no phase shifts were observed, indicating there were no environmental changes to hydrogen and therefore no structural changes to the chemical contents in tea [18,19]. This is important as any slight changes to the chemical structure might not produce the same health effects [18]. As tea contains more than thirty thousand compounds, it is crucial to understand that tea processing does not change chemical structures and is safe for human consumption [1].

Comparing Bao Chong tea under 45°, 75°, and 90°C brewing water

Tea is valued not only for its taste, but also for its antioxidant content, which can bring health benefits. Besides the production of tea, temperature of the brewing water could also cause great differences in the taste of tea or even the released compounds. Based on the results of this study, the best temperature for brewing tea to produce caffeine,

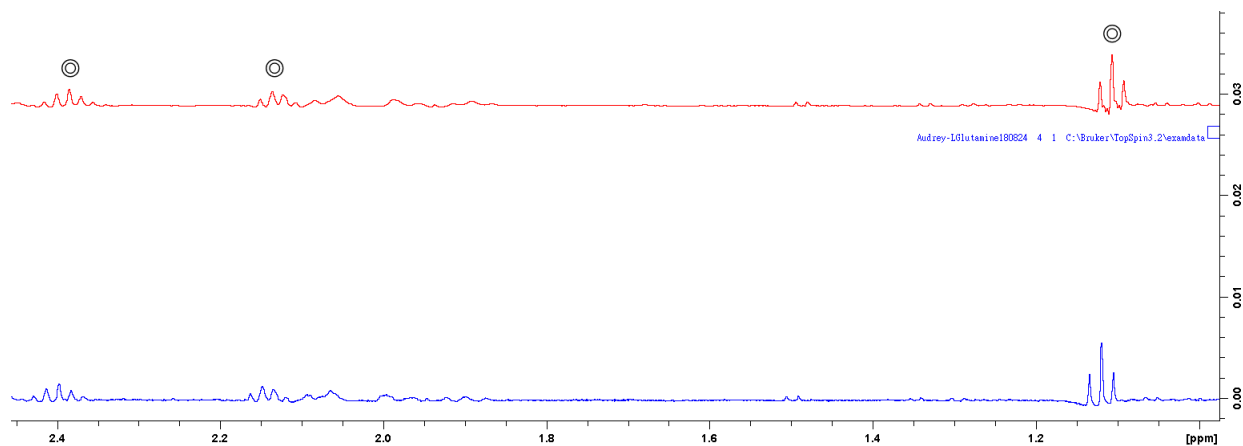


Figure 4. 0 to 2.5 ppm NMR spectra of 25°C and 45°C Bao Chong Tea. Spectra represent brewing temperatures 25°C [red] and 45°C [blue]. Corresponding peaks are denoted by ■ [caffeine], ▲ [catechins], and circle [L-theanine].

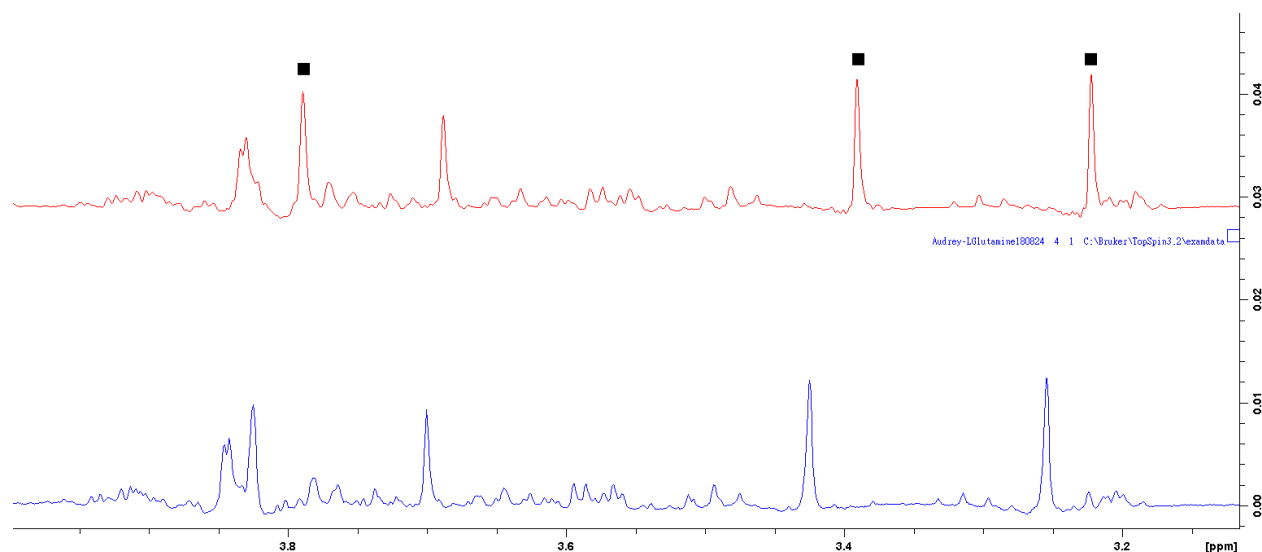


Figure 5. 3.1 to 4.0 ppm NMR of 25°C and 45°C Bao Chong Tea. Spectra represent brewing temperatures of 25°C [red] and 45°C [blue]. Corresponding peaks are denoted by ■ [caffeine], ▲ [catechins], and circle [L-theanine].

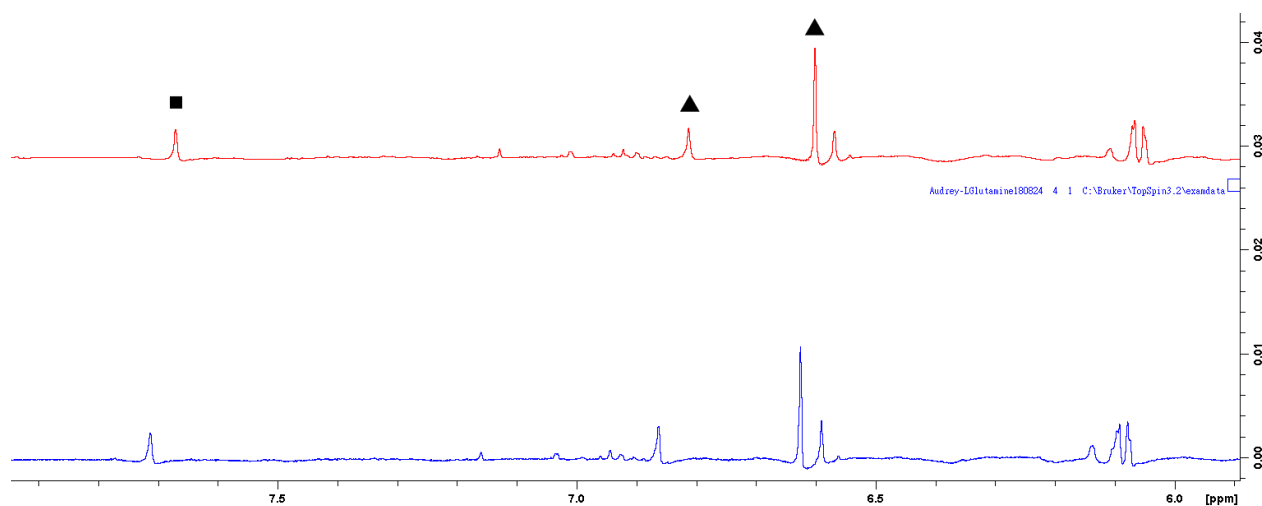


Figure 6. 6.0 to 8.0 ppm NMR of 25°C and 45°C Bao Chong Tea. Spectra represent brewing temperatures of 25°C [red] and 45°C [blue]. Corresponding peaks are denoted by ■ [caffeine], ▲ [catechins], and circle [L-theanine].

catechins and L-theanine was between 45°C and 75°C. Caffeine, catechins and L-theanine levels remained the same for 45°C to 75°C but reduced greatly when the temperature increased to 90°C (**Figure 3, Table 1**). The varying amounts of compounds in the tea when brewed with different water temperatures might be due to the fact that there are certain ranges of temperatures that are best for the compounds to be released [20-22].

However, the literature suggests that the optimum conditions to extract L-theanine is 80°C, 85°C for catechins, and 90°C or 100°C for caffeine [20-22]. This difference might be due to different measuring methods. For further research, various types of tea could be brewed at different temperatures, followed by analysis of the levels of different compounds.

Another finding in this study was that the caffeine and catechins peaks shifted upfield to different amounts for 45°C and 75°C compared to 90°C (**Figure 3**). Also, the shifting pattern of the caffeine peak to 7.60 ppm is unordered (**Figure 3**). The shifting peaks might indicate slight changes in the NMR magnetic field or changes in concentration or additives [19]. It could be concluded that there were hydrogen related environmental changes, but the compound itself did not change [19]. Since the shifting was not appreciable, it can be assumed that the changes were minimal [19]. Further investigation is required to identify the nature of the changes that occurred.

All the peaks that do not indicate caffeine, catechins and L-theanine represent different compounds found in tea. There were not many significant changes observed for those other peaks besides the area between 5.20 ppm to 5.40 ppm, which is suspected to be sugar, indicating that most compounds were not sensitive to brewing water temperature (**Figure 3**) [12]. An explanation to this could be that sugar becomes very sensitive to molecular changes when it reaches around 90°C and will be released greatly at 90°C. However, an in-depth literature search found no supporting evidence to prove or disprove the explanation, so this could be a direction for future research.

Comparing Bao Chong tea under 25° and 45°C brewing water

Cold-brewed tea is also a common drink and can be made easily by immersing tea leaves in bottled water for 12 hours [13]. Therefore, this experiment aimed to compare 25°C and 45°C brewing water. However, the experiment between 25°C and 45°C Bao Chong tea is distinct from the previous two because the two samples were prepared differently. The 25°C trial used tea leaves that were immersed for 12 hours, while the 45°C trial used tea leaf powder that was immersed for 3 minutes. Thus, the outcome cannot be attributed to the temperature change.

Although the 25°C and 45°C trials differed by their preparation, the changes were noteworthy. The amount of caffeine increased, catechins decreased, and L-theanine remained the same from 25°C to 45°C (**Figure 2**). The

general pattern remained as well, indicating that the length of time which tea leaves are immersed in water will not affect the overall contents in the tea. However, there are two independent variables in this experiment, which makes the cause of the changes uncertain. Therefore, future research could compare 25°C and 45°C brewing temperature for the same amount of time, or brewing tea at the same temperature for various amount of times. This would clarify the changes within this experiment.

Additionally, shifted peaks were found for caffeine, catechins, and L-theanine (**Figures 4-6**). The shifting peaks indicate changes in NMR magnetic field, concentration, or additives [19]. This could be due to different temperatures or brewing time. However, a more in-depth investigation is required to better understand the reason behind the changes.

A structural difference at 3.8 ppm was also found (**Figure 5**). The compound was suspected to be caffeine or a type of catechin [12]. It is a conformational change, which means the changes in the environment have caused changes in shape of the macromolecule [23]. Although most of the changes seen in this experiment may be caused by external variations such as hydrogen related environmental changes, the compound at 3.8 ppm had structural changes because of its sensitivity towards temperature. This sensitivity might be due to the compound structure where the hydrogens in caffeine compounds are more widely spread compared to the unchanged L-theanine and are more easily affected by water temperature.

Besides the limitations mentioned in previous sections, there are also possible errors within this research. Only one trial was conducted for each water temperature, and the lack of replication might lead to unidentified errors. The measurements made during the experiment might contain random errors because of the variable measurements, including the milligram balance, pipet, and the NMR machine. The temperature control during the experiment is unstable because it is controlled by a hot plate without a precise temperature and was monitored by a thermometer, causing the temperature of the water to be variable. Therefore, a few improvements for future research include conducting more trials of the same temperature to ensure accuracy and reduce errors, using a hot plate with a temperature control along with a covered beaker, and other additions when brewing water to prevent heat loss. Another aspect to improve upon in future research is the NMR set up. NMR spectra can be highly accurate when all the sources of errors are properly addressed [24]. The get-prosol would need to be set correctly to get the probe head and solvent to the corresponding acquisition parameter [25]. Moreover, the number of scans would need to be set appropriately to ensure the level of accuracy, and the relaxation times would need to be long enough for the spectrometer to adjust measurements in order to produce accurate results [24]. To ensure that the collected data was accurate, various setting conditions should be conducted and the results should be compared to ensure the outcomes are the same [24].

Specific future investigations could be performed on the basis of this research. Various brands of tea could be tested to investigate if the result is suitable regardless of the brand. Samples can be analyzed using other NMR techniques such as ^{13}C -NMR or ^{15}N -NMR or the two-dimensional nuclear magnetic resonance spectroscopy (2D NMR) to offer a more precise understanding of the structural change of caffeine, catechins and L-theanine. A more comprehensive investigation can be conducted by extracting the compounds in the tea for more accurate comparison. A brewing water temperature comparison could be conducted on different types of tea, for example, green tea or black tea. Also, the relationship between brewing time and the number of times tea leaves are brewed and the levels of chemicals that make up tea content can be investigated. Additionally, how the environmental conditions of tea farms affect chemical contents of tea could also be studied. Various types of compounds and their correlation with brewing water temperature, types of tea, brewing time could also be investigated. For example, specific types of catechins such as EGCG and ECG, various kinds of sugar, or flavanols such as kaempferol and quercetin glycoside [21], could all be future research topics.

In conclusion, drinking Bao Chong tea was suggested to be more beneficial than green tea or black tea as it has the highest content of the investigated compounds, where black tea has the lowest for all. Therefore, Bao Chong tea could be selected to drink if the consumer is looking to drink tea for its health benefits. Also, brewing water between 45°C and 75°C was suggested as the best for releasing caffeine, catechins, and L-theanine. Therefore, in the future, people could measure their tea brewing water temperature and make tea according to their desired beverages. Lastly, although a relationship between caffeine, catechins, and L-theanine and 25°C and 45°C brewing water cannot be drawn directly, there are significant changes in the NMR results which require future investigation.

METHODS

^1H NMR is a technology used to detect the different hydrogen environments in the compound [25]. By using NMR, the changes in compounds caused by the different brewing temperatures can be detected.

Preparation for tea samples

Green tea, Bao Chong tea, and black tea leaves, depending on the experiment, were first ground into powder and 100mg was measured and transferred into an Eppendorf tube. Distilled water was added into a second Eppendorf tube and placed into a beaker with water and “cooked” on a hot plate for ten minutes after reaching the desired temperature (75°C for tea type comparison and 45°C , 75°C , and 90°C for temperature comparison). 1.2 mL of cooked distilled water was taken from the second Eppendorf tube and added into the Eppendorf tube with tea powder as mentioned above, and the Eppendorf tube with tea powder was then put into the

same beaker and “cooked” on the hot plate for three minutes. After that, the Eppendorf tube was removed from the beaker and put into a centrifuge for ten minutes. After centrifugation, 0.4 mL of the supernatant liquid was extracted and mixed with 0.1 mL of D_2O in an NMR tube. NMR samples were vortexed for thirty seconds before being placed into a 500Hz NMR to be analyzed.

Preparation for Bao Chong tea under 25°C brewing water

An extra trial of 25°C was prepared the day before the experiment. 1g of tea leaves was added to 600 mL of water for 12 hours [13].

The use of NMR

To compare the different chemical contents of tea under various conditions, proton nuclear magnetic resonance spectroscopy (^1H NMR) was utilized. Access to this technology was provided by the Department of Chemistry at Academia Sinica. The set-up of NMR was as listed: the solvent selected as D_2O , the acquisition time set as 0.5 per second, the number of scans set as 128, time domain data size set as 5000, and spectra width in hertz set as 5000.

NMR peak integration

After combining the NMR spectra, the magnifications were increased on a computer for measurements. A ruler was used to measure the length of the desired peaks. After that, peaks of the same temperature were divided by the smallest measure and written as a ratio.

Received: April 8, 2018

Accepted: February 28, 2019

Published: May 14, 2019

REFERENCES

1. Tadesse, Alemu et al. “Quantification of Total Polyphenols, Catechin, Caffeine, L-Theanine, Determination of Antioxidant Activity and Effect on Antileishmanial Drugs of Ethiopian Tea Leaves Extracts.” *Pharmacognosy Research*, vol. 7, no. 5, 2015, p. 7., doi:10.4103/0974-8490.157991.
2. Gebely, Tony. “What Is Oxidation.” *World of Tea*, 15 Feb. 2012, worldoftea.org/tea-leaves-oxidation/.
3. “Tea Processing Steps: Eli Tea Processing Chart.” *Eli Tea Detroit USA, Eli Tea*, 2013, www.eliteabar.com/blogs/tea-education/7780719-tea-processing.
4. McGee, Harold. “Iced Coffee and Tea: (Not) Taking the Heat.” *The New York Times*, 19 July 2011, nyti.ms/2sGXnJx.
5. Steinmann, Joerg et al. “Anti-infective properties of epigallocatechin-3-gallate (EGCG), a component of green tea.” *British Journal of Pharmacology*, vol. 168, no. 5, 2013, doi: 10.1111/bph.12009.
6. Nathan, Pradeep J., et al. “The Neuropharmacology of

- L-Theanine(N-Ethyl-L-Glutamine).” *Journal of Herbal Pharmacotherapy*, vol. 6, no. 2, 2006, pp. 21–30., doi:10.1080/j157v06n02_02.
7. Nobre, Anna. “L-Theanine, a Natural Constituent in Tea, and Its Effect on Mental State.” *Asia Pacific of Clinical Nutrition*, vol. 17, 2008.
 8. National Center for Biotechnology Information. “Caffeine.” PubChem Compound Database. CID=2519.
 9. Tzou, Der Lii. Personal Interview, 13 Jan. 2018.
 10. National Center for Biotechnology Information. “L-Theanine.” PubChem Compound Database. CID=439378.
 11. “Green Tea May Lower Heart Disease Risk.” Harvard Health Publishing, Harvard Medical School, Dec. 2012.
 12. Gall, Gwénaëlle Le, et al. “Metabolite Profiling Using 1H NMR Spectroscopy for Quality Assessment of Green Tea, *Camellia sinensis*(L.)” *Journal of Agricultural and Food Chemistry*, vol. 52, no. 4, 2004, pp. 692–700., doi:10.1021/jf034828r.
 13. Feng, Teng Guang. Personal Interview, 29 May. 2017.
 14. Drake, Christopher, et al. “Caffeine Effects on Sleep Taken 0, 3, or 6 Hours before Going to Bed.” *Journal of Clinical Sleep Medicine*, vol. 9, no. 11, 2013, doi:10.9737/hist.2018.658.
 15. Khokhar, Santosh, and Magnusdottir. “Total Phenol, Catechin, and Caffeine Contents of Teas Commonly Consumed in the United Kingdom.” *Journal of Agricultural and Food Chemistry*, vol. 50, no. 3, 2002, pp. 565–570., doi:10.1021/jf010153l.
 16. Temple, Norman J. *Beverage Impacts on Health and Nutrition*. Edited by Ted Wilson, 2nd ed., 2016.
 17. Boros, Klára, et al. “Theanine and Caffeine Content of Infusions Prepared from Commercial Tea Samples.” *Pharmacy Magazine*, vol. 12, no. 45, 2016, doi: 10.4103/0973-1296.176061
 18. “Measurements and data processing.” *Chemistry: Course Companion*, by Sergey Bylikin et al., Oxford University Press, 2014, pp. 283–285.
 19. Wu, Dani. Personal Interview, 13 January. 2018.
 20. Vuong, Quan, et al. “Optimum Conditions for the Water Extraction of L-Theanine from Green Tea.” *Journal of Separation Science*, vol. 34, no. 18, 2011, doi: 10.1002/jssc.201100401
 21. Nhan, Pham Phuoc, and Nguyen Tran Phu. “Effect of Time and Water Temperature on Caffeine Extraction from Coffee.” *Pakistan Journal of Nutrition*, vol. 11, no. 2, 2012, pp. 100–103., doi: 10.3923/pjn.2012.100.103.
 22. Saklar, Sena, et al. “Effects of Different Brewing Conditions on Catechin Content and Sensory Acceptance in Turkish Green Tea Infusions.” *Journal of Food Science and Technology*, vol. 52, no. 10, 2015, pp. 6639–6646., doi:10.1007/s13197-015-1746-y.
 23. Wahyuni, D. S. C., et al. “NMR Metabolic Profiling of Green Tea (*Camellia sinensis* L.) Leaves Grown at Kemuning, Indonesia.” *Journal of Physics: Conference Series*, vol. 795, 2017, p. 012013., doi:10.1088/1742-6596/795/1/012013.
 24. “How to Reduce 1H NMR Evaluation Errors.” Anasazi Instruments, 21 Aug. 2018, aiinmr.com/nmr-spectroscopy-q-a-blog/reducing-1h-nmr-quantitative-evaluation-errors/.
 25. “Basic Acquisition Parameters: The ‘Eda’ Table.” AVANCE Beginners Guide, Instituto De Química Física Rocasolano Departamento De Química Física Biológica., 2003, [triton.iqfr.csic.es/guide/man/beginners/chap7-5.htm](http://iqfr.csic.es/guide/man/beginners/chap7-5.htm).

Copyright: © 2019 Lin, Tzou, and Ponnampalam. All JEI articles are distributed under the attribution non-commercial, no derivative license (<http://creativecommons.org/licenses/by-nc-nd/3.0/>). This means that anyone is free to share, copy and distribute an unaltered article for non-commercial purposes provided the original author and source is credited

Financial Support: Thanks to JEI Sponsor Alloy Therapeutics for support of this article’s publication..

The effect of ultraviolet radiation and the antioxidant curcumin on the longevity, fertility, and physical structure of *Drosophila melanogaster*: Can we defend our DNA?

Shan Lateef*, Delaney Walts*, and LaRina Clark

Benton Middle School, Manassas, VA

*authors contributed equally

SUMMARY

Ultraviolet (UV) radiation is known to alter DNA structure and impair cellular function in all living organisms. One proposed mechanism of injury involves the production of harmful free radicals. The DNA damage caused by UV radiation can lead to a myriad of medical issues, but there is limited research on potential rescue interventions. However, studies have suggested that naturally occurring antioxidants may exert their positive influence on an organism by reducing oxidative injury, which leads to the purpose of this project: to study the effects of UV radiation and determine whether antioxidant-enriched nutrition can combat the potential deleterious effects of UV radiation on *Drosophila melanogaster*. We hypothesized that UV radiation would diminish the lifespan and fertility of *Drosophila*, as well as causing physical abnormalities. We also predicted that *Drosophila* cultured in the presence of media enriched with the antioxidant curcumin would have enhanced lifespans and fertility. Finally, we hypothesized that raising *Drosophila* with curcumin-enriched media, would diminish the negative impact of UV radiation on the organism's longevity and fertility. We found that UVB (320nm) radiation caused a 59% decrease in the *Drosophila* lifespan and mutagenic effects on flies' physical appearance, but did not significantly affect fertility. Curcumin significantly prolonged lifespan and enhanced fertility for both UV- and non-UV-exposed flies. Therefore, we conclude that curcumin can prolong lifespan, enhance fertility, and mitigate the deleterious effects of UV radiation on *Drosophila*. Our research demonstrates that we can harness the positive potential of natural antioxidants and use them as weapons in our war against radiation-induced diseases, including conditions like cancer.

INTRODUCTION

The genetic code, inscribed in the DNA of each species, is vital to the unique and efficient functioning of every living organism [1]. However, this genetic code is not securely protected. External forces may influence our genetic instructions and cause devastating diseases such as cancer. One such environmental force is ultraviolet (UV) radiation,

which is on the rise due to depletion of atmospheric ozone [2]. Ultraviolet radiation can cause both direct and indirect damage to the DNA of living organisms [3]. Cells do have some repair mechanisms to fix the damage, but these pathways are not always completely successful [3]. For example, the form of UV radiation known as UVB (290-320 nm wavelength), can damage living cells and alter the molecular structure of DNA by causing physical breaks or mutations in DNA structure [4], a phenomenon that is implicated in carcinogenesis. UV radiation can also cause indirect DNA damage by creating free radicals. Free radicals are molecules that are highly reactive due to the presence of unpaired electrons. Such hydroxyl radicals can attack the DNA backbone and bases, potentially causing cells to die or develop mutations. [3]. By causing damage to cells and DNA, free radical build-up can lead to cancer and other diseases.

Just as the environment can negatively influence our genetic information, some naturally occurring protective factors have also been identified. One such tool is a set of compounds called antioxidants [5]. Endogenous antioxidants are those which living organisms may produce for the sole purpose of neutralizing free radicals by donating electrons while exogenous antioxidants are extracted from external sources such as food and supplements. Beta-carotene, lycopene, and vitamins A, C, and E are primary forms of exogenous antioxidants. Studies in the 1990s reported that individuals with a low intake of antioxidant-rich food were at a greater risk for developing chronic diseases, including cancer [5]. However, studies that looked at the relationship between antioxidants and conditions like cardiovascular disease and cancer did not find convincing evidence for antioxidants' protective effects. It is important to note, however, that those trials were of short duration, were conducted in people with existing diseases, and utilized artificially manufactured antioxidant supplements [5].

Prior research has looked at UV-radiation-induced DNA damage in animal models, including *Drosophila melanogaster*, or the simple fruit fly, and shown that such radiation can have harmful effects on flies' lifespan, fertility and physical structure [6, 7]. Research has also shown that antioxidants such as curcumin can extend the *Drosophila* lifespan [8]. *Drosophila* also has a short, simple reproductive cycle lasting about 8-14 days, so several generations can be observed in

weeks [8]. Curcumin is a natural, organic antioxidant found in turmeric, a spice which is consumed and used for medicinal purposes in Asia [9]. Curcumin has been shown to scavenge free radicals such as the superoxide anion and to exhibit anti-cancer properties [9].

Based on a thorough review of the scientific literature, we posed the following questions: If UV radiation damages DNA at least in part by creating free radicals, and antioxidants are effective neutralizers of those free radicals, can we use one agent to protect us from the harmful effects of the other? If an organism is provided with antioxidant-rich nutrition, will this diet make it less likely to succumb to the harmful effects of UV radiation? To our knowledge, these questions have never been answered by the scientific community. We chose to study these questions using *Drosophila melanogaster* for several reasons. They are small and inexpensive to maintain, and 75% of the genes that cause disease in humans are also found in the fruit fly [10].

We designed an experiment to study the effects of UV radiation and antioxidant-enriched nutrition on *Drosophila* and to study whether the potential beneficial effects of antioxidant treatment can mitigate the harmful effects of UV radiation. We hypothesized that: 1) flies exposed to UV radiation will show reduced lifespan and fertility, as well as physical abnormalities; 2) flies cultured with curcumin-enriched media will show increased lifespan and fertility; and 3) flies cultured with curcumin-enriched media will be protected against the negative impact of UV radiation on longevity and fertility. As a result of these experiments, we concluded that treatment with the antioxidant curcumin increases the fertility of fruit flies, both in UV- and non-UV-exposed flies. UV radiation caused devastating mutagenic effects to the physical structure in both parent and offspring generations, including tumors and crippling wing mutations. UV radiation also caused a significant decrease in lifespan, but this effect was counteracted by treatment with curcumin. Additionally, curcumin treatment increased *Drosophila* lifespan and even had the ability to mitigate the effect of UV radiation on lifespan. Therefore, curcumin has the ability to act as a preventative measure against ultraviolet radiation and resulting health risks in flies.

RESULTS

We placed *Drosophila* cultures into four experimental groups: control, UV-exposure only, curcumin-enriched media only, and UV exposure with curcumin-enriched media. The UV group was exposed to UVB (320 nm) radiation in a dark room for three minutes. We transferred flies into fresh vials every four days and recorded numbers of alive flies. To assess fertility, we anesthetized flies and separated them by sex. Five flies of each sex were placed into each vial. We used the same four experimental groups. We then counted the larvae and pupae on days 5 and 10 similar to previously published methods [6]. To study physical structure, 4-5 flies were anaesthetized and their physical characteristics were

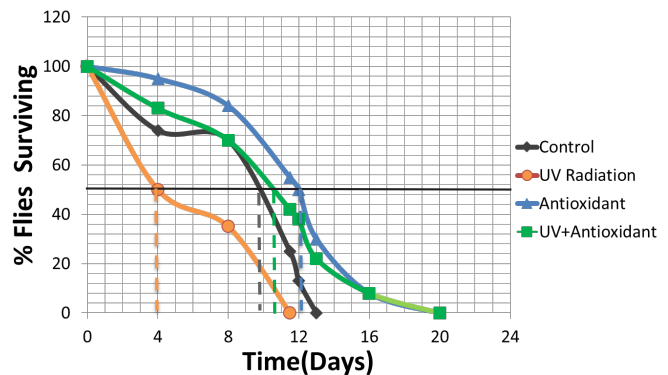


Figure 1. *Drosophila* longevity of all experimental groups. This graph displays the relative survival rates for all experimental groups as well as the 50% Cohort Survival (n = 20-25 flies per vial). UV radiation alone caused a significant decrease in lifespan, which was associated with an extremely steep slope. The antioxidant nutrition was somewhat able to mitigate this effect.

observed. After UV exposure, we examined flies for any mutagenic effects on both first and second generations.

At each time point studied, the antioxidant group did the best in terms of survival and the UV-exposed group did the worst (Figure 1, Table 1). Importantly, flies that were given curcumin-enriched media but were also exposed to UV radiation lived longer than control flies, but not as long as those who were given the same media but not exposed to radiation. This demonstrates that the antioxidant was able to partially protect the *Drosophila* from radiation-induced injury.

We assessed fertility by counting larvae and pupae on days 5 and 10. By day 10, the antioxidant group had many more offspring (mean = 44.7, SEM = 21.1) than either the control (mean = 7.0, SEM = 3.2) or UV-exposed (mean = 8.7, SEM = 3.5) groups (Table 2, Figures 2-3). On day 10, we also observed that the UV + antioxidant group (mean =

Experimental Condition	Days
No UV, no antiox	9.7
+UV only	4.0
+Antioxidant only	10.5
+Antioxidant, +UV	12.0

Table 1. Time taken for 50% of flies to die.

Experimental Condition	Mean (Std Error)	
	Day 5	Day 10
	Larvae & pupae	Larvae & pupae
No UV, no antiox	0.7 (0.58)	7.0 (3.21)
+UV only	0.3 (0.33)	8.7 (3.48)
+Antioxidant only	3.7 (1.40)	44.7 (21.07)
+Antioxidant, +UV	1.7 (1.67)	40.0 (22.01)

Table 2. Effect of UV radiation and curcumin of *Drosophila* fertility.

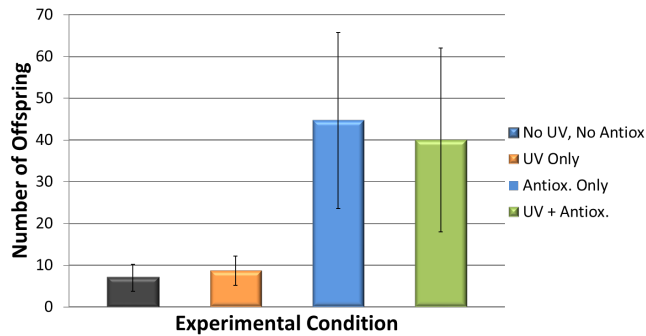


Figure 2. Fertility results on day 10 . Shown here is the average number of offspring (larvae/pupae) per experimental group on Day 10. UV radiation did not influence fertility. However, antioxidant nutrition significantly enhanced fertility in flies with and without exposure to UV radiation. (5 male and 5 female flies per vial)

40.0, SEM = 22.0) had greater survival than the control or UV-only groups (Table 2, Figure 2-3). We also found that the *Drosophila* that were raised on antioxidant-rich media had far more pupae than those without. In summary, UV radiation did not significantly decrease the reproductive potential of *Drosophila*. We also found that antioxidant treatment led to an increased number of offspring, even in flies exposed to UV radiation, but this effect was not statistically significant ($p = 0.2464$, two-way ANOVA).

In terms of physical structure, *Drosophila* exposed to UV radiation showed a darkened exoskeleton. The offspring of UV-exposed flies showed many more mutagenic effects (Figure 4), including vestigial and curved wing structures, which are well-established mutations that map to chromosome 2 [11]. We also found abnormal head growths and tumors. In addition, we observed that second-generation larvae and pupae had very translucent body chambers compared to the more-opaque controls, perhaps making them more susceptible to environmental insults.

DISCUSSION

The purpose of this experiment was to determine the effects of UV radiation and antioxidant (curcumin)-rich nutrition on the phenotype of *Drosophila melanogaster*, as well as to assess whether antioxidant treatment could diminish the harmful effects of UV radiation on the organism. Our hypotheses were partially supported by our results. UV radiation appeared to decrease *Drosophila* lifespan based on the form of the longevity curves, however, this was not subjected to a test of statistical significance. UV radiation did cause mutagenic effects on their physical structure. However, UV radiation did not decrease the fertility of *Drosophila*. Antioxidant-rich nutrition, in the form of curcumin-enriched media, appeared to increase *Drosophila* lifespan and fertility but the latter effect was not statistically significant. Although not subject to statistical testing, our data suggested that curcumin treatment may enable UV-exposed flies to live much longer than both flies who only received UV radiation and control flies. Lastly, curcumin treatment increased the number of larvae and pupae

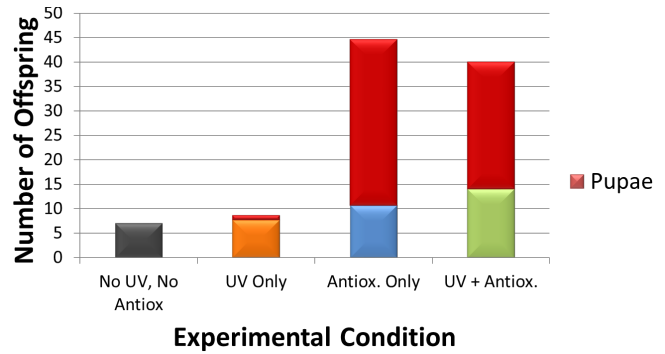


Figure 3. Fertility-larvae and pupae day 10. This figure displays the distribution of offspring among larvae and pupae for each experimental group. The antioxidant nutrition groups seemed to have an accelerated life cycle with more pupae present on day ten compared to larvae. (5 male and 5 female flies per vial)

produced, even after the flies been exposed to UV radiation. We recognize that our quantitative data is preliminary and not subject to rigorous statistical testing, however, it does suggest an interesting trend it terms of the harmful effects of UV radiation and the potentially beneficial effects of the antioxidant, curcumin. Due to the fact that *Drosophila* share 75% of the genes that cause diseases in humans, the data collected in this experiment would be clinically relevant to a degree, but with some discrepancies due to the natural differences between *Drosophila* and humans. A clinical trial or further research in mammalian systems would be useful in order to solidify the validity between our data and its effects on humans.

The decrease in *Drosophila* lifespan due to UV radiation may be caused by DNA damage and the induction of cancer, as has been previously described [10]. It could also reflect

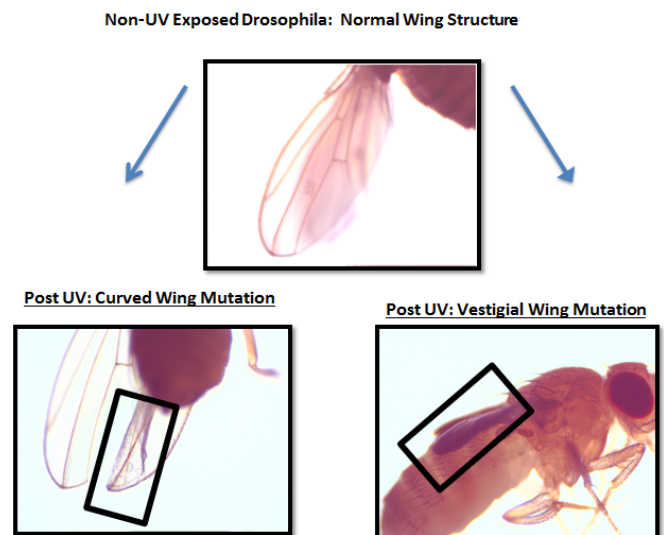


Figure 4. The effects of UV radiation on *Drosophila* physical structure. These figures display the phenotypic effects of UV radiation on *Drosophila*. Dichaite and vestigial wing mutations (in the F1 generation) were produced in response to exposure (n = 15-20 flies per group).

tissue injury and aging mechanisms caused by excessive free radical production [11]. Prolongation of lifespan by curcumin supports prior literature [9], and our data shows, for the first time, that this naturally-derived antioxidant can even mitigate the negative effects on lifespan induced by UV radiation. UV radiation did not affect *Drosophila* fertility, possibly indicating that the rays did not affect gonadal cells or that the DNA repair mechanisms within the reproductive system were more proficient. Antioxidant treatment may enhance fertility, perhaps by increasing the overall health and vigor of the organism and also indirectly by prolonging lifespan and allowing a longer reproductive time frame. UV radiation produced mutagenic effects on the *Drosophila* physical structure as previously described, especially with regards to wing development [7].

Our findings are extremely exciting and promise a potential breakthrough in the prevention of radiation-induced diseases such as cancer. Our research demonstrates that we can utilize the positive potential of natural antioxidants in our war on cancer. It is possible that antioxidants exert their positive effects by protecting against injury within various organ systems and by scavenging mutation-causing free radicals, which can be formed naturally or under the influence of radiation. The findings of our study have broad implications for the design of preventive approaches against environmental hazards such as UV radiation. Clinical research and human studies are vital to furthering our understanding of this protective phenomenon and its applicability to public health. It would also be extremely informative to study the effect of antioxidant dosages and determine a minimum and maximum effective dosage, as well as toxicity at large doses if applicable.

Our study is limited by a small number of fruit flies, due to space and budget limitations. Future studies should analyze the corresponding DNA changes associated with the phenotypic effects so that we can better understand carcinogenesis. Research in this field is critically necessary to help scientists design novel prevention strategies for devastating diseases, including cancer. While we must continue pursuing research to find a cure for cancer, we should be equally committed to stopping cancer before it even gets started.

METHODS

Experiment 1: Dependent Variable = Longevity

Wild-type *Drosophila melanogaster* were acquired from Carolina Biological Company and maintained at room temperature under normal lighting conditions. Eight vials of culture media were prepared and labeled, two for each of the following experimental conditions: 1) No UV exposure or curcumin treatment; 2) UV exposure only; 3) curcumin treatment; and 4) UV exposure and curcumin treatment. Four vials contained curcumin-enriched culture medium (100 mg curcumin/1 g culture medium). USDA-certified organic curcumin was obtained from Micro Ingredients Company. 15-20 *Drosophila* were placed in each vial.

A 4-watt (254/354 nm) UV lamp was used to irradiate two experimental groups (UV only and UV + antioxidant) in a dark room for three minutes. All vials were placed in a small incubator and maintained at a temperature of 25-28°C. The adult flies were transferred to new vials every four days to avoid including their offspring in the longevity count. During each transfer, we recorded the dead flies in the old vial, living flies in new vial, and the percentage of flies remaining alive in each of the experimental groups. Data were tabulated and graphed on survival curves.

Experiment 2: Dependent Variable = Fertility

Twelve vials of culture media were prepared and labeled, three for each of the four experimental groups described above. Six vials contained curcumin-enriched culture medium (1 mg curcumin/1 g culture medium). A *Drosophila* Kit from Carolina Biological was obtained in which sex is matched to eye color: red-eyed flies were female and white-eyed flies were male. Flies were carefully anaesthetized using FlyNap (Carolina Biological) and separated into two groups by gender. Five male and five female flies were placed into each vial. Six vials were irradiated as described above. The larvae and pupae were counted in each vial five and 10 days after UV exposure. Mean offspring and standard error were calculated for each group, and developmental distribution of offspring was noted.

Experiment 3: Dependent Variable = Physical Structure

We examined 4-5 wild-type fruit flies under a microscope for characteristics such as body shape, eye color, and wing anatomy. Microscopic photographs were taken in order to document the standard physical structure. From the same wild-type culture, we collected flies to set up four vials, two each for no-UV and for UV-exposed *Drosophila*. Two vials were exposed to UV radiation as described above. We observed flies for the next three-to-four weeks. After one week, when larvae became visible, we transferred the parental generation to a new vial and studied these flies for physical abnormalities. After three weeks, we studied the second generation for mutagenic effects. Again, we used the FlyNap anesthetic to immobilize the flies so that they could be observed and photographed under the microscope.

ACKNOWLEDGEMENTS

We would like to thank Dr. Tara Lateef for her mentorship throughout this entire process, as well as Mrs. Amy Massman for her unending support and encouragement throughout our scientific journey. We also greatly appreciate our principal, Mrs. Huebner, for supporting all STEM efforts at our school.

Received: October 24, 2018

Accepted: April 30, 2019

Published: May 18, 2019

REFERENCES

1. Pray, L. "Discovery of DNA structure and function: Watson and Crick." *Nature Education*, vol. 1, no. 1, 2008, gbe.ius.edu.ba/sites/default/files/u796/discovery_of_dna_structure_and_function.pdf. Accessed 27 Aug. 2018.
2. "Stratospheric ozone depletion, UV radiation and health." World Health Organization, www.who.int/globalchange/ozone_uv/en/. Accessed 27 Aug. 2018.
3. Ravanat, J., et al. "Direct and indirect effects of UV radiation on DNA and its components." *Journal of Photochemistry and Photobiology B: Biology*, 22 Oct. 2001, doi:10.1016/S1011-1344(01)00206-8.
4. Sinha, R., and D. Häder. "UV-induced DNA damage and repair: a review." *Photochemical & Photobiological Sciences*, 13 Mar. 2002, pp. 225-36, doi:10.1039/B201230H.
5. "Antioxidants: Beyond the Hype." *The Nutrition Source*, www.hsph.harvard.edu/nutritionsource/antioxidants/. Accessed 27 Aug. 2018.
6. ZhePeng, W., et al. "Phototoxic effect of UVR on wild type, ebony and yellow mutants of *Drosophila melanogaster*: Life Span, fertility, courtship and biochemical aspects." *Science in China Series C-Life Sci*, vol. 51, no. 10, Oct. 2008, pp. 885-93, doi:10.1007/s11427-008-0085-5.
7. Negishi, T., et al. "Somatic-cell mutation induced by UVA and monochromatic UV radiation in repair-proficient and -deficient *Drosophila melanogaster*." *Photochemistry and Photobiology*, vol. 73, no. 5, 6 Feb. 2001, pp. 493-98, doi:10.1562/0031-8655(2001)073<0493:SCMIBU>2.0.CO;2.
8. Suckow, B., and M. Suckow. "Lifespan Extension by the Antioxidant Curcumin in *Drosophila Melanogaster*." *International Journal of Biomedical Science*, vol. 2, no. 4, Dec. 2006, pp. 402-05, www.ncbi.nlm.nih.gov/pmc/articles/PMC3614642/.
9. Aggarwal, B., et al. "Anticancer potential of curcumin: preclinical and clinical studies." *Experimental Therapeutics*, Jan.-Feb. 2003, pp. 363-98. <http://www.ncbi.nlm.nih.gov/pubmed/12680238>. Accessed 27 Aug. 2018
10. Pandey, U. B., and C. D. Nichols. "Human disease models in *Drosophila melanogaster* and the role of the fly in therapeutic drug discovery." *Pharmacological reviews*, 63(2), 2011, 411-36.
11. Bridges, C. B. "Current Maps of the Location of the Mutant Genes of *Drosophila Melanogaster*" *Proceedings of the National Academy of Sciences of the United States of America* vol. 7,4 (1921): 127-32.
12. Fleming, J., et al. "Role of oxidative stress in *Drosophila* aging." *Mutation Research/DNAging*, vol. 275, nos. 3-6, 5 Feb. 2003, pp. 267-79, doi:10.1016/0921-8734(92)90031-J.

are distributed under the attribution non-commercial, no derivative license (<http://creativecommons.org/licenses/by-nc-nd/3.0/>). This means that anyone is free to share, copy and distribute an unaltered article for non-commercial purposes provided the original author and source is credited.

Financial Support: Thanks to JEI Sponsor Alloy Therapeutics for support of this article's publication.

The effect of caffeine on the regeneration of Brown Planaria (*Dugesia tigrina*)

Olivia Lazorik¹, Michael Lazorik²

¹Phillips Exeter Academy, Exeter, New Hampshire

²St. Lucie County School District, Fort Pierce Florida (retired)

SUMMARY

Planaria are considered the most primitive form of cephalized animal with similarity to vertebrate nervous systems. They possess nearly every neurotransmitter present in most mammals, including dopamine. Planaria are known for their extraordinary ability to regenerate from a small tissue fragment, making planaria an ideal model to study the nervous system. Planaria have pluripotent somatic stem cells known as neoblasts. Following amputation, neoblasts increase their rate of return and migrate to the wound site. They then give rise to a mass of new tissue called the blastema. Cells in the blastema differentiate over a period of several days to replace missing body structures. Previous research compared scoring methods of neurotoxicity on the neurological, locomotive, and morphological functions of planarian. High levels of dopamine have been found in regenerating planaria, indicating that dopamine may have a role in regeneration. Caffeine enhances dopamine signaling in the brain. Therefore, this study aimed to explore the effect of caffeine on the regeneration rate of planaria. In this study, twenty-one planaria were exposed to two concentrations of caffeine. The heads were amputated, and regeneration was recorded by digital photography. The study showed that the highest dosage of caffeine accelerated the regeneration rate of the planaria in comparison to the lower dosage and control. The planaria treated with the lower caffeine dosage also regenerated in less time than the control specimen. This study is evidence that a high dose of caffeine accelerates planaria regeneration and implicates caffeine as a possible treatment to stimulate the regeneration process.

INTRODUCTION

Degeneration, or death of nerve cells, results in movement and mental functioning problems. These symptoms, commonly observed in Parkinson's patients, are a result of the dopaminergic neuron death in the substantia nigra region of the brain. As the disease progresses, motor skills and mental acuity decline. The National Parkinson Foundation estimates that over 10 million people worldwide suffer from Parkinson's disease. With 60,000 people diagnosed annually in the United States, it is estimated that by 2020 more than 1 million Americans will be living with Parkinson's disease (1). It is

generally accepted by the scientific community that neurogenesis is evident in many areas of the brain, including the hippocampus (2). However, the ability to regenerate neurons varies amongst species and diminishes most significantly in the human brain as it matures. Given the hippocampus and striatum govern long-term memory and cognitive skills, respectively, evidence of the ability to regenerate nerve cells, although limited, in these regions is a promising area for continued research that may benefit patients suffering from neurodegenerative diseases (2).

Since research suggests that neurons in humans may regenerate, the use of models with regeneration capabilities may be useful for the study of neurodegenerative diseases like Parkinson's. The central nervous system of planaria consists of a bi-lobed brain connected to a pair of nerve cords that extend ventrally from the head (3) and has extensive regeneration capabilities. In fact, all parts of the planarian can regenerate, even from a fragment as small as 1/279th of the organism's original size (4). Regeneration in planaria is caused by pluripotent stem cells distributed throughout the body, which give rise to all cell types (4). High levels of dopamine have been extracted from regenerating planarian, suggesting that dopamine has a role in the regeneration process (5). In addition, planaria share with vertebrates all the major developmental signaling pathways of cells (4). Regions of the planarian genome have been identified as having significant similarity to human disease-related genes (3). These commonalities, along with ease of maintenance and cost-effectiveness of husbandry, make planaria an excellent test model. By studying the regeneration process in this system, we can learn how to positively impact neurogenesis.

Caffeine is an alkaloid compound commonly found in coffee, tea, and cacao and is used medicinally as a stimulant and diuretic. Caffeine enhances dopamine signaling in the brain by antagonizing adenosine receptors (6). Studies of planaria treated with caffeine solutions have had varying results. In a study at East Tennessee State University, researchers found that levels of caffeine greater than 0.01 M were toxic to planaria after three days of exposure to the treatment (7). Measures of survivorship in this study also showed that after three days, 60% of the planaria died in the 1000 μ M solution, while 50% died in the 100 μ M solution (7). All planaria survived at a caffeine concentration of 10 μ M (7). Another study suggested that 10 μ M caffeine accelerates the stages of regeneration starting with blastema development, growth, and differentiation when compared to a control treatment of

spring water (8). Because planaria react to their environmental conditions using chemical, mechanical, and light sensory neurons, data can be collected on these cells to assess the effect of treatments.

The goal of this research was to determine the ability of caffeine to accelerate the regeneration of pluripotent planarian cells. Considering dopamine has found in high levels during planaria regeneration and caffeine enhances dopamine signaling, we hypothesize that the caffeine treatment will decrease the time for planaria to regenerate after amputation. For the purpose of this study, amputation was performed immediately below the head to separate the bi-lobed brain from the ventral nerve cord. The number of days from amputation to full regeneration was assessed through visual inspection. The purpose of the research is to investigate the usage of caffeine as a treatment to stimulate regeneration.

RESULTS

We measured the time to full regeneration of amputated planarian in three experimental groups: control, low caffeine dose (30 μM) and high caffeine dose (60 μM). To measure the rate of regeneration, the head of each planarian was amputated to separate the bi-lobed brain from the nerve cord that extends ventrally from the head. Every 24 hours, a photo was taken of each planarian, the photo was analyzed, and the stage of regeneration was recorded. The time required for each specimen to reach each stage of regeneration was recorded and averaged across the experimental group. This allowed us to calculate the average regeneration elapsed time (in days) for each stage in each experimental group (Figure 1).

The results indicate the high caffeine group accelerated the time (7.88 days) to reach full regeneration in comparison to the low caffeine (7.70 days) and control (7.76 days) groups.

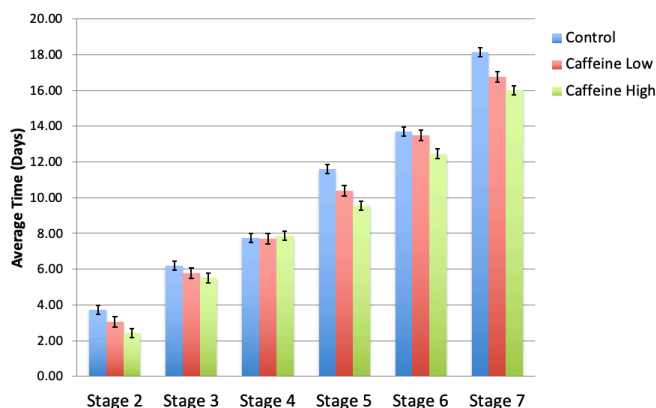


Figure 1. Average time to reach each regeneration stage by experimental group. Each planarian was inspected to determine the stage of regeneration. The average for each experimental group by stage was calculated and the standard error determined. The high caffeine dose accelerated all regeneration stages except stage 4. The low caffeine dose accelerated the regeneration in stages when compared to the control group.

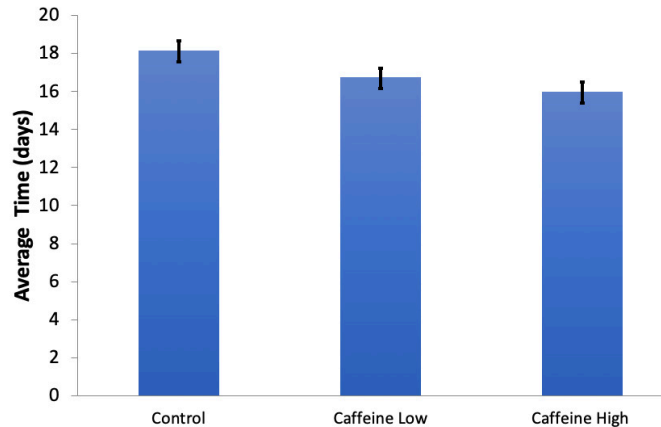


Figure 2. Average time to reach full regeneration by experimental group. Each planarian was inspected to determine the final stage of regeneration, stage 7. The high caffeine reached stage seven in the shortest period of time of 16.0 days \pm 1.0699 (60 μM ; $p=0.0225$, one-way ANOVA); low caffeine in 16.74 days \pm 1.3495 (30 μM ; $p=0.1894$, one-way ANOVA), and control in 18.15 days \pm 1.549.

The high caffeine group accelerated the time to reach all regeneration stages, except stage 4. Planaria treated with low caffeine reached all regeneration stages in less time than control specimens

We calculated the average time to full regeneration for each experimental group by taking the duration in days from amputation to the first observation that a planarian reached stage 7. Planaria in the high caffeine group regenerated more quickly than planaria in the control group (Figure 2). The average regeneration time for the caffeine high group was 16 days, 2.15 days shorter than the control time of 18.15 days, reflecting an 11.8% increase in regeneration rate ($p=0.0225$). We found no difference in the average regeneration time between the control and caffeine low treatment groups ($p=0.1804$). The difference in regeneration speed between caffeine high versus caffeine low was 0.74 days, or a 4.4% increased rate in the low caffeine treatment group; this difference was not statistically significant ($p=0.6777$).

As studies have shown, caffeine may have a positive or negative effect on planaria depending on dosage. Previous studies indicated fatalities at a dosage level of 0.01 M. This study compared the dosage of 30 μM to 60 μM of caffeine and found that the higher dosage accelerated planaria regeneration without fatalities.

DISCUSSION

The results support our hypothesis that a caffeine treatment stimulates regeneration by decreasing the time required for planaria to regenerate following amputation below the bi-lobed brain. Each planarian was amputated below the head and visually inspected to determine that the amputation was completed within the guidelines. The regeneration stage was assessed based on the presence of developmental milestones for each stage of regeneration, as documented

in the material and methods section. Based on the average time it took each planarian to reach stage 7 (full regeneration), we found that the caffeine low group (30 μ M; $p=0.1804$) did not regenerate more quickly than the control group. However, the planaria treated with a high dose of caffeine (60 μ M; $p=0.0225$) regenerated in 11.8% less time and 2.14 fewer days as compared to the control group. As planaria regenerate completely in 16-18 days, this represents a substantial increase in regeneration rate. These findings also suggest that regeneration in planaria was affected by the caffeine dosage, as only the higher dosage (60 μ M) of caffeine had caused a significant increase in the rate of planaria regeneration.

Caffeine, a widely consumed psychoactive substance, works in the nervous system; it enhances dopamine signaling by slowing down dopamine reabsorption in the human brain. Previous studies support that planaria have dopaminergic receptors in their nervous system, and high levels of dopamine have been extracted from regenerating planaria. (9) Planaria absorb chemicals such as caffeine by epithelial diffusion or intake the chemicals through their pharynx. This has been demonstrated in pharmaceutical toxicology testing utilizing spectrophotometry (10). Caffeine is metabolically active in the planarian, as it has been found to increase planarian motility in a concentration-dependent manner, a behavioral effect consistent with findings in vertebrates (6).

Planaria maintain a large population of pluripotent stem cells. This study suggests that caffeine accelerates the regeneration and differentiation of these pluripotent cells into neural cells. Stem cell therapy for patients suffering from Parkinson's disease involves injecting stem cells directing into the basal ganglia, in hopes that these cells will differentiate into dopaminergic neurons. Caffeine may promote cell regeneration and neuronal differentiation in that context, as well, potentially improving therapeutic outcomes for patients with neurodegenerative disease.

MATERIALS AND METHODS

Brown Planaria (*Dugesia tigrina*), a common freshwater representative of the phylum Platyhelminthes, was used in this experiment. The planaria were obtained from a commercial source, Carolina Biological Supplies ($n=21$). Kaffn8 liquid caffeine was used as the caffeine source. Three temporary holding containers were filled with spring water (Poland Spring Water) and seven planaria were assigned to each holding container. One gram of egg yolk was placed into each

holding container as food. After 24 hours, residual egg yolk was removed.

The experiment began with creating two caffeine concentration solutions (30 μ M and 60 μ M). Petri dishes (90 x 15 mm) were labeled to identify the treatment, and each petri dish was filled with 15 mL of the treatment per their label. Each planarian was transferred from the holding container to a petri dish filled with spring water tracked with a unique identifier (labeled with numbers 1-21). A baseline photo was taken of each planarian using a digital camera on macro mode. After all photos were taken, each planarian was randomly assigned to a treatment group and placed into the associated treatment petri dish. The unique tracking number and treatment association was recorded. After 24 hours, each planarian was amputated by cutting the planarian slightly below its head with an X-Acto knife as it stretched to move. Post-amputation, each planarian was inspected to validate that the amputation was performed immediately below the head. The residual planarian (body without head) was placed back in the petri dish. The head section was placed in the surplus stock holding container (one for each environment).

To track the regeneration stages, a photo of the planarian in an elongated position was taken every 24 hours with a digital camera in macro mode (Figure 3). The photo was visually inspected, and the stage of development was recorded as follows: 1. Pre-wound closure - no visible regrowth to fill gap from wound closure, 2. Wound closure - cut has flattened and started to regrow, 3. Pattern formation - wound closed and round, formation visible, 4. Head translucent, but visible, 5. Head still mostly translucent, shape starting to peak, early photoreceptors now visible, 6. Head and photoreceptors visible, but still more translucent than rest of body, 7. Head fully peaked, photoreceptors visible, head color same as the remainder of body

The visual inspection was not blinded given the naming convention. However, the model reference stage pictures minimized potential bias.

The planaria were fed every seven days with one gram of cooked egg yolk. Any excess yolk was removed from each petri dish after two hours. At the conclusion of the experiment, the planaria had the opportunity to live out their natural lifespan.

The data was analyzed utilizing the statistical functions of Excel. The one-way ANOVA comparisons test was performed using GraphPad Prism (GraphPad Software, La Jolla

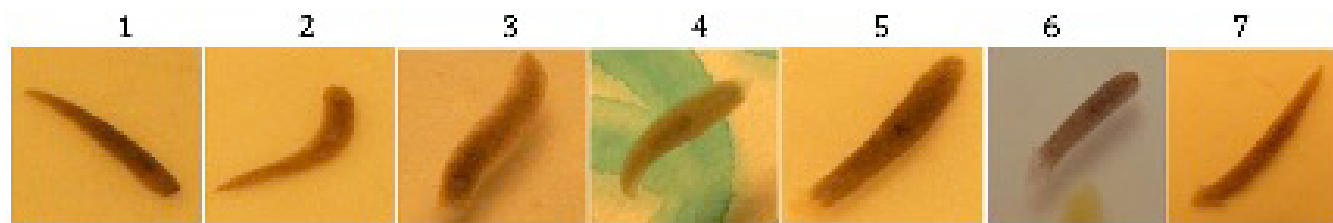


Figure 3. Planaria regeneration score reference. Representative images of planaria taken in an elongated position every 24 hours in macro mode.

California USA).

ACKNOWLEDGEMENTS

I would like to thank my mother, Lori Lazorik, for procuring the required supplies, helping me record the data, and reviewing my submission.

Received: August 30, 2018

Accepted: March 24, 2019

Published: May 10, 2019

REFERENCES

1. "Statistics." Parkinson's Foundation, 28 Mar. 2019, www.parkinson.org/Understanding-Parkinsons/Statistics. Accessed 21 April 2019.
2. Sorrells, Shawn F, et al. "Human Hippocampal Neurogenesis Drops Sharply in Children to Undetectable Levels in Adults." *Nature*, Vol. 55, 2018, pp. 377-381
3. Gentile, L., et al. "The Planarian Flatworm: An In Vivo Model for Stem Cell Biology and Nervous System Regeneration." *Disease Models & Mechanisms*, vol. 4, no. 1, 2010, pp.12–19., doi:10.1242/dmm.006692
4. Sánchez Alvarado, Alejandro. "Q&A: What is regeneration, and why look to planarians for answers?" *BMC Biology*, BioMed Central, Vol. 10, No. 88, 2012
5. Rangiah, Kannan, and Dasaradhi Palakodeti. "Comprehensive Analysis of Neurotransmitters from Regenerating Planarian Extract Using an Ultrahigh Performance Liquid Chromatography/Mass Spectrometry/ Selected Reaction Monitoring Method." *Rapid Communications in Mass Spectrometry*, vol. 27, no. 21, 2013, pp. 2439–2452., doi:10.1002/rcm.6706.
6. Pagán, Oné R et al. "The flatworm planaria as a toxicology and behavioral pharmacology animal model in undergraduate research experiences" *Journal of undergraduateneuroscience education: JUNE: a publication of FUN, Faculty for Undergraduate Neuroscience* vol. 7, no. 2, 2009, pp A48-52.
7. Collins, Erica Leighanne. "The Effect of Caffeine and Ethanol on Flatworm Regeneration." *Digital Commons @ East Tennessee State University*, dc.etsu.edu/etd/2028/. Accessed 21 April 2019.
8. Kwon, Diane, and Joel Tatum. "Comparison of Planarian (*Dugesia tigrina*) Regeneration Rate in Caffeine and Aloe Vera Solutions." https://www.saddleback.edu/faculty/steh/bio3bfolder/3BPPTs/Kwon_Tatum%20-%20Bio%203B%20PPT%20Presentation.pdf
9. Nishimura, Kaneyasu, et al. "Regeneration of Dopaminergic Neurons after 6-Hydroxydopamine-Induced Lesion in Planarian Brain." *Journal of Neurochemistry*, Vol 119, No. 6, 2011, pp. 1217-1231
10. Hagstrom, Danielle, et al. "Planarian Brain Regeneration as a Model System for Developmental Neurotoxicology." *Regeneration*, vol. 3, no. 2, 2016, pp. 65–77., doi:10.1002/reg2.52.
11. Pohanka, M. "The Perspective of Caffeine and Caffeine Derived Compounds in Therapy." *Bratislava Medical Journal*, vol. 116, no. 09, 2015, pp. 520–530., doi:10.4149/blj_2015_106. www.ncbi.nlm.nih.gov/pubmed/26435014.
12. Borota, Daniel, et al. "Erratum: Corrigendum: Post-Study Caffeine Administration Enhances Memory Consolidation in Humans." *Nature Neuroscience*, vol. 17, no. 9, 2014, pp. 1287–1287., doi:10.1038/nn0914-1287a.
13. Shomrat, T., and M. Levin. "An Automated Training Paradigm Reveals Long-Term Memory in Planarians and Its Persistence through Head Regeneration." *Journal of Experimental Biology*, vol. 216, no. 20, Feb. 2013, pp. 3799–3810., doi:10.1242/jeb.08780.
14. Volkow, ND et al. "Caffeine increases striatal dopamine D2/ D3 receptor availability in the human brain" *Translational Psychiatry* vol. 5, no. e549, 2015, doi:10.1038/tp.2015.46

Copyright: © 2019 Lazorik and Lazorik. All JEI articles are distributed under the attribution non-commercial, no derivative license (<http://creativecommons.org/licenses/by-nc-nd/3.0/>). This means that anyone is free to share, copy and distribute an unaltered article for non-commercial purposes provided the original author and source is credited.

Financial Support: Thanks to JEI Sponsor Alloy Therapeutics for support of this article's publication.

Sponsorship



Editor's Circle

\$10,000+



Patron

\$5,000+



PORTFOLIOS
WITH PURPOSE®

Institutional Supporters



HARVARD
UNIVERSITY



HARVARD
MEDICAL SCHOOL



Tufts
UNIVERSITY

Charitable Contributions

We need your help to provide mentorship to young scientists everywhere.

JEI is supported by an entirely volunteer staff, and over 90% of our funds go towards providing educational experiences for students. Our costs include manuscript management fees, web hosting, creation of STEM education resources for teachers, and local outreach programs at our affiliate universities. We provide these services to students and teachers entirely free of any cost, and rely on generous benefactors to support our programs.

A donation of \$30 will sponsor one student's scientific mentorship, peer review and publication, a six month scientific experience that in one student's words, 're-energized my curiosity towards science', and 'gave me confidence that I could take an idea I had and turn it into something that I could put out into the world'. **If you would like to donate to JEI, please visit <https://emerginginvestigators.org/support>, or contact us at questions@emerginginvestigators.org.** Thank you for supporting the next generation of scientists!

'Journal of Emerging Investigators, Inc. is a Section 501(c)(3) public charity organization (EIN: 45-2206379). Your donation to JEI is tax-deductible.'



emerginginvestigators.org